EUROPEAN ORGANIZATION FOR NUCLEAR RESEARCH (CERN)

CERN-EP-2023-132
2024/06/05

CMS-HIG-21-011

Search for a new resonance decaying into two spin-0 bosons in a final state with two photons and two bottom quarks in proton-proton collisions at $\sqrt{s} = 13\,\text{TeV}$

The CMS Collaboration*

arXiv:2310.01643v2 [hep-ex] 3 Jun 2024

Abstract

A search for a new boson X is presented using CERN LHC proton-proton collision data collected by the CMS experiment at $\sqrt{s} = 13\,\text{TeV}$ in 2016–2018, and corresponding to an integrated luminosity of $138\,\text{fb}^{-1}$. The resonance X decays into either a pair of Higgs bosons HH of mass 125 GeV or an H and a new spin-0 boson Y. One H subsequently decays to a pair of photons, and the second H or Y, to a pair of bottom quarks. The explored mass ranges of X are 260–1000 GeV and 300–1000 GeV, for decays to HH and to HY, respectively, with the Y mass range being 90–800 GeV. For a spin-0 X hypothesis, the 95% confidence level upper limit on the product of its production cross section and decay branching fraction is observed to be within 0.90–0.04 fb, depending on the masses of X and Y. The largest deviation from the background-only hypothesis with a local (global) significance of 3.8 (below 2.8) standard deviations is observed for X and Y masses of 650 and 90 GeV, respectively. The limits are interpreted using several models of new physics.

Published in the Journal of High Energy Physics as doi:10.1007/JHEP05(2024)316.

© 2024 CERN for the benefit of the CMS Collaboration. CC-BY-4.0 license

*See Appendix A for the list of collaboration members

1 Introduction

With the discovery of a Higgs boson H in 2012 at the CERN LHC by the ATLAS and CMS Collaborations [1–3], the standard model (SM) has proven to describe most observed phenomena up to the TeV scale [4–9]. However, some of the important aspects of nature are left outside of this theory, such as dark matter and the nature of gravity. Beyond-SM (BSM) theories have been proposed to address these shortcomings, and many of these predict the existence of new massive spin-0 and -2 particles.

Among the BSM theories, models with "warped extra dimensions" (WEDs) [10, 11] postulate the existence of an additional spatial dimension in which the carriers of a quantized gravitational force (gravitons) propagate. In addition, according to the "Randall–Sundrum bulk model", matter particles are also allowed to propagate in the extra dimension. This model contains massive resonances, the spin-0 radion [12–14] and spin-2 bulk gravitons (excited modes of the gravitational field each separated by a characteristic mass scale) [15–17], which have sizable branching fractions for decaying into HH [18]. For this model, the fundamental scale is the reduced Planck scale $\overline{M_{pl}}$ with ultra-violet cutoff Λ_{R} [12]. In the specific range of model parameters considered for this analysis, a narrow-width approximation is permitted for the resonances [18].

Supersymmetry (SUSY) is an extension of the SM which postulates a fermion-boson pairing symmetry (superpartners) [19, 20]. The minimal supersymmetric SM (MSSM) extends the SM Lagrangian by introducing an extra complex scalar doublet [21, 22]. The next-to-minimal supersymmetric SM (NMSSM) [23, 24] introduces one additional complex singlet field, and is the most straightforward supersymmetric extension to the SM where the electroweak scale originates from the SUSY-breaking scale. The NMSSM could provide a natural solution to the "unnaturalness" problem of MSSM [25], wherein the difference between the m_{H} and the Planck scale is of many orders of magnitude. In the NMSSM Higgs-sector, several spin-0 bosons exist, one of which can be associated with the H discovered so far. More massive spin-0 bosons may decay to the lighter ones in this model.

Similar to the NMSSM, a model with two real scalar singlet fields (TRSM), in addition to the SM Higgs field, has been proposed [26]. The mixing between the Higgs doublet and these additional scalar fields gives three massive scalar bosons, one of which can be identified as the SM-like H. This model, too, allows the heavier scalar to decay into lighter scalars.

Motivated by the above BSM scenarios, this paper presents the search for a massive particle X decaying either to HH or to H and another spin-0 boson Y, using LHC proton-proton (pp) collision data collected by the CMS experiment in 2016–2018 at $\sqrt{s} = 13\,\mathrm{TeV}$ and corresponding to a total integrated luminosity of $138\,\mathrm{fb}^{-1}$. The results are interpreted within the framework of the BSMs presented above.

The search is performed in the final state with a pair of photons γ and bottom b quarks ($\gamma\gamma\mathrm{b\bar{b}}$). Figure 1 shows a tree-level Feynman diagram of the signal process. In using this channel, the $\mathrm{X} \to \mathrm{HH}$ search benefits from the combination of the $\mathrm{H} \to \gamma\gamma$ decay, with its relatively large signal purity, and the $\mathrm{H} \to \mathrm{b\bar{b}}$ decay, with its large branching fraction. For the H, the SM decay branching fractions [27] are assumed. The HY search is independent of any assumption on the $\mathrm{Y} \to \mathrm{b\bar{b}}$ branching fraction.

The analysis uses a strategy similar to the search for nonresonant production of HH in the $\gamma\gamma\mathrm{b\bar{b}}$ final state [28, 29]. One H candidate is reconstructed from a pair of photons $\gamma\gamma$, with their invariant mass $m_{\gamma\gamma}$ compatible with m_{H}. The candidate for the second boson, either H or Y, is reconstructed from a pair of b jets (particle jets originating from the fragmentation

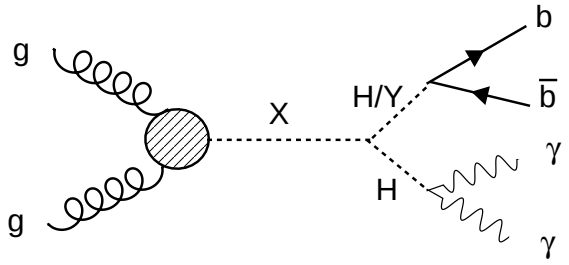

Figure 1: Feynman diagram showing a tree-level gluon-gluon fusion production of a BSM resonance X decaying to a pair of spin-0 bosons (HH or HY), which then decay to the $\gamma\gamma b\bar{b}$ final state.

and hadronization of b quarks), with their invariant mass m_{jj} compatible with m_H or with an assumed value of the Y boson mass m_Y. Events are selected using machine learning algorithms to suppress background contributions. The signal is extracted from a two-dimensional (2D) maximum likelihood fit spanning the ($m_{\gamma\gamma}$,m_{jj}) plane.

This paper is organized as follows: Section 2 provides a brief description of the CMS detector followed by the details of the data and simulated event samples in Section 3. The analysis strategy is discussed in Section 4, including background rejection methods along with the signal and background modeling studies. Section 5 details the systematic uncertainties. The results are presented in Section 6, and the analysis is summarized in Section 7. Tabulated results are provided in the HEPData record for this analysis [30].

2 The CMS detector

The central feature of the CMS apparatus is a superconducting solenoid of 6 m internal diameter, providing a magnetic field of 3.8 T. Within the solenoid volume, there is a silicon pixel and strip tracker, a lead tungstate crystal electromagnetic calorimeter (ECAL), and a brass and scintillator hadron calorimeter (HCAL), each composed of a barrel and two endcap sections. Forward calorimeters extend the pseudorapidity η coverage provided by the barrel and endcap detectors. Muons are measured in gas-ionization detectors embedded in the steel flux-return yoke outside the solenoid. A more detailed description of the CMS detector, together with a definition of the coordinate system used and the relevant kinematic variables, can be found in Ref. [31].

Events of interest are selected using a two-tiered trigger system [32]. The first level (L1), composed of custom hardware processors, uses information from the calorimeters and muon detectors to select events at a rate of around 100 kHz within a fixed latency of about 4 μs [33]. The second level, known as the high-level trigger, consists of a farm of processors running a version of the full event reconstruction software optimized for fast processing and reduces the event rate to around 1 kHz before data storage [34].

The global event reconstruction, also called particle-flow (PF) event reconstruction [35], aims to reconstruct and identify each individual particle in an event (PF candidates), with an optimized combination of all subdetector information. In this process, the identification of the particle type (photon, electron, muon, charged or neutral hadron) plays an important role in the determination of the particle direction and energy.

Photons are identified as ECAL energy clusters not linked to the extrapolation of any charged particle trajectory to the ECAL. Electrons are identified as a primary charged particle track and

potentially many ECAL energy clusters corresponding to this track extrapolation to the ECAL and to possible bremsstrahlung photons emitted along the way through the tracker material. Muons are identified as tracks in the central tracker consistent with either a track or several hits in the muon system, and associated with calorimeter deposits compatible with the muon hypothesis. Charged hadrons are identified as charged particle tracks neither identified as electrons, nor as muons. Finally, neutral hadrons are identified as HCAL energy clusters not linked to any charged hadron trajectory, or as a combined ECAL and HCAL energy excess with respect to the expected charged hadron energy deposit.

The energy of photons is obtained from the ECAL measurement. The raw ECAL energy is corrected in data using a multivariate analysis (MVA) based regression which is trained on Monte Carlo (MC) simulation of $\mathrm{Z} \to \mathrm{ee}$ events. In the simulated events, the energy of the photons is smeared to match the resolution in data [36, 37]. For photon identification, an MVA identification method (photon ID) based on photon shower shape, isolation, and kinematic variables is used [36].

The energy of electrons is determined from a combination of the track momentum at the main interaction vertex, the corresponding ECAL cluster energy, and the energy sum of all bremsstrahlung photons attached to the track [38]. The energy of muons is obtained from the corresponding track momentum. The energy of charged hadrons is determined from a combination of the track momentum and the corresponding ECAL and HCAL energies, corrected for the response function of the calorimeters to hadronic showers. Finally, the energy of neutral hadrons is obtained from the corresponding corrected ECAL and HCAL energies. In the barrel section of the ECAL, an energy resolution of about 1% is achieved for unconverted or late-converting photons in the tens of GeV energy range. The energy resolution of the remaining barrel photons is about 1.3% up to $|\eta| = 1$, changing to about 2.5% at $|\eta| = 1.4$. In the endcaps, the energy resolution is about 2.5% for unconverted or late-converting photons, and between 3 and 4% for the other ones [39]. The $m_{\gamma\gamma}$ resolution, as measured in $\mathrm{H} \to \gamma\gamma$ decays, is typically in the 1–2% range, depending on the measurement of the photon energies in the ECAL and the topology of the photons in the event [40].

For each event, jets are clustered from these reconstructed particles using the infrared and collinear safe anti-k_{T} algorithm [41, 42] with a distance parameter of 0.4. Jet momentum is determined as the vectorial sum of all particle momenta in the jet, and is found from MC simulations to be, on average, within 5–10% of the true value over the whole transverse momentum p_{T} spectrum and detector acceptance. Additional pp interactions within the same or nearby bunch crossings (pileup) can contribute additional tracks and calorimetric energy depositions to the jet momentum. To mitigate this effect, charged particles identified to be originating from pileup vertices are discarded and an offset correction is applied for the remaining neutral particle contributions [43]. Corrections, derived from MC simulations, are applied in order to bring the measured jet energies to that of the originating particles, on average. Furthermore, in situ measurements of the momentum balance in dijet, γ+jet, Z+jet, and multijet events are used to account for any residual differences in the jet energy scale between data and MC simulations [44]. An additional energy correction algorithm based on machine learning techniques is applied in this analysis to further improve the jet energy scale of b jets [45].

The jet energy resolution amounts typically to 15–20% at 30 GeV, 10% at 100 GeV, and 5% at 1 TeV [44]. Additional selection criteria are applied to each jet to remove jets potentially dominated by anomalous contributions from various subdetector components or reconstruction failures.

The missing transverse momentum vector $\vec{p}_{\mathrm{T}}^{\,\mathrm{miss}}$ is computed as the negative vector p_{T} sum

of all the PF candidates in an event, and its magnitude is denoted as p_T^{miss} [46]. The $\vec{p}_T^{miss}$ is modified to account for the corrections to the energy scale of the reconstructed jets in the event.

3 Data and simulated samples

The data used in this analysis were collected by the CMS detector from LHC pp collisions at $\sqrt{s} = 13\,\text{TeV}$ in 2016–2018. The total analyzed data correspond to an integrated luminosity of $138\,\text{fb}^{-1}$ [47–49]. Events are collected using the trigger condition for the year 2016 (2017–2018) that requires two photons with thresholds $p_T^{\gamma_1} > 30\,\text{GeV}$ and $p_T^{\gamma_2} > 18\ (22)\,\text{GeV}$ and with $m_{\gamma\gamma} > 90\,\text{GeV}$, where γ_1 and γ_2 represent leading- and subleading-p_T photons, respectively. The photons in the trigger algorithm have also to satisfy requirements on their calorimeter shower shapes, on the ratio of their energies deposited in the HCAL to that in the ECAL (identification variable), and on the p_T carried by charged hadrons in the vicinity of the photon candidate (isolation requirement) [36].

MC simulations of resonant production of X via gluon-gluon fusion (ggF), with subsequent decays, assuming a narrow-width approximation, to either HH or HY were generated at next-to-leading order (NLO) using the MADGRAPH5_aMC@NLO package [50, 51]. For the WED-motivated searches for spin-0 and -2 resonances, the MADGRAPH5_aMC@NLO package versions were 2.2.2 and 2.4.2, for the 2016 and 2017–2018 simulated samples, respectively. The signals were generated for m_X in range 260–1000 GeV. For the NMSSM-motivated searches, the signal samples were generated using MADGRAPH5_aMC@NLO 2.6.5 for $300 < m_X < 1000\,\text{GeV}$ and for $90 < m_Y < 800\,\text{GeV}$. The samples were generated in steps of 100 GeV in m_X, and the kinematic mass distributions for intermediate m_X were modeled by interpolating the shape parameters of the above simulated samples. Within signal simulations, a value of 125 GeV is assumed for m_H.

The upper bound for m_X search at 1 TeV is defined by the transition toward the Lorentz-boosted regime, where particles resulting from the hadronization of both b quarks merge into a single jet. The upper range of m_Y is set by the energy-momentum conservation rule for the on-shell particles $m_Y \leq m_X - m_H$. Below $m_Y = 90\,\text{GeV}$, the search capabilities are limited by the position of the kinematic turn-on in the m_{jj} distribution [28, 29].

The dominant backgrounds include the SM nonresonant multijet processes with up to two prompt photons, either as the irreducible $\gamma\gamma$+jets events or the reducible γ+jets events. The $\gamma\gamma$+jets background is modeled with SHERPA 2.2.1 [52] at leading order (LO) and includes up to three additional partons at the matrix element level. The γ+jets background is modeled with PYTHIA 8.212 [53] at LO. The nonresonant background simulations are used only in the optimization and validation of the background estimation method using an MVA-based discriminator.

Single H productions, where the H decays to $\gamma\gamma$, are considered as resonant backgrounds. These background events give a signal-like resonant distribution for $m_{\gamma\gamma}$, which is one of the observables in the analysis. The ggF H is simulated at NLO using POWHEG 2.0 [54–57]. The vector-boson fusion production (VBF H) and production in association with top quark pairs ($t\bar{t}H$) are simulated at NLO using MADGRAPH5_aMC@NLO v2.2.2 (2016) or v2.4.2 (2017–2018). The H production in association with a vector boson (VH) and in association with b quarks ($b\bar{b}H$) [58] are simulated using MADGRAPH5_aMC@NLO v2.6.1. The cross sections and decay branching fractions are taken from Ref. [27]. The SM nonresonant HH production has a negligible contribution within the analysis phase-space and is not explicitly considered as a separate background source.

The simulated samples are interfaced with PYTHIA for parton showering and fragmentation with the standard p_T-ordered parton shower scheme. The underlying event is modeled with PYTHIA, using the CUETP8M1 (CP5) tunes for 2016 (2017–2018) [59, 60]. Parton distribution functions (PDFs) are taken from the NNPDF3.0 [61] NLO (2016) or NNPDF3.1 [62] next-to-NLO (2017–2018) except for the LO simulations, for which the PDF4LHC15_NLO_MC set at NLO [61, 63–66] is used. The detector response is modeled using the GEANT4 [67] toolkit. The simulated event samples also include a similar pileup as observed in the data, with an average of 23 (32) pp interactions per bunch crossing in 2016 (2017–2018) data.

4 Analysis strategy

4.1 Object reconstruction and event preselections

Photons are considered if they are contained within the ECAL and tracker fiducial region of $|\eta| < 2.5$, excluding the ECAL barrel-endcap transition region ($1.44 < |\eta| < 1.57$), and they also need to pass the selections $p_T^{\gamma_1}/m_{\gamma\gamma} > 1/3$, $p_T^{\gamma_2}/m_{\gamma\gamma} > 1/4$, and $100 < m_{\gamma\gamma} < 180\,\text{GeV}$. The primary pp vertex associated with the diphoton system is identified using an MVA technique [68]. The efficiency of the correct vertex assignment is 99.9%, aided by the requirement of at least two jets in the $\gamma\gamma b\bar{b}$ final state.

The jets are required to be within the tracker fiducial volume, so that track information can be used to identify heavy flavor (b and c) jets. These jets must have $p_T > 25\,\text{GeV}$ and $|\eta| < 2.4$ (< 2.5) for 2016 (2017–2018), while also passing jet identification criteria, in order to reject spurious jets from calorimeter noise [69]. The $|\eta|$ selection of jets is looser for the 2017–2018 data-taking years because of the installation of the new pixel detector at the beginning of 2017 [70]. Then, the jets and photons are required to be separated by $\Delta R \equiv \sqrt{(\Delta\eta)^2 + (\Delta\phi)^2} > 0.4$, where $\Delta\eta$ and $\Delta\phi$ are the pseudorapidity and the azimuthal angle (measured in radians) differences between a photon and the closest jet, respectively. This selection is used in order to avoid counting of photons as jets. Finally, jet pairs with $70 < m_{jj} < 190$ (1200) GeV for HH (HY) analysis are retained for further selection, respectively.

For the identification of b jets, a deep neural network (DNN) score-based tagger DEEPJET [71–73] is used. It utilizes information related to tracks and secondary vertex of b jets. The pair with the highest sum of DEEPJET discriminant scores in the event is selected as a H (Y) candidate. If no such pair is present, the event is rejected. The physics object reconstruction and event preselection criteria are summarized in Table 1. The signal efficiency varies from 30–60%. For HH searches, it increases with m_X. In HY searches, for a fixed m_Y the signal efficiency increases with m_X, but, for a fixed m_X it decreases with m_Y.

The X candidate is reconstructed from the selected pairs of photons and jets. Figure 2 shows the $m_{\gamma\gamma}$, m_{jj}, and 4-body invariant mass $m_{\gamma\gamma jj}$ distributions in the data and MC simulations after the full set of selection criteria. The best estimate of the mass of the X candidate is given by the variable $\widetilde{M}_X$, which has a better resolution than $m_{\gamma\gamma jj}$ [74] because of the resolution subtraction of $m_{\gamma\gamma}$ and m_{jj}, defined as:

$$\widetilde{M}_X \equiv m_{\gamma\gamma jj} - (m_{\gamma\gamma} - m_H) - (m_{jj} - m_{H\text{ or }Y}) \quad (1)$$

The improvement in resolution by using $\widetilde{M}_X$ instead of $m_{\gamma\gamma jj}$ ranges from 30% at high m_X up to 90% at low m_X.

Table 1: Event preselection criteria.

Photons		Jets	
Variable	Requirement	Variable	Requirement
Leading photon p_T	$> m_{\gamma\gamma}/3$	p_T	> 25 GeV
Subleading photon p_T	$> m_{\gamma\gamma}/4$	$\Delta R_{\gamma j}$	> 0.4
$\lvert\eta\rvert$	< 2.5	$\lvert\eta\rvert$	< 2.4 (2.5) for 2016 (2017–2018)
		Number of jets	> 1
$m_{\gamma\gamma}$	100–180 GeV	m_{jj}	70–190 (70–1200) GeV for HH (HY)
			Jet-pair with the highest DEEPJET score sum

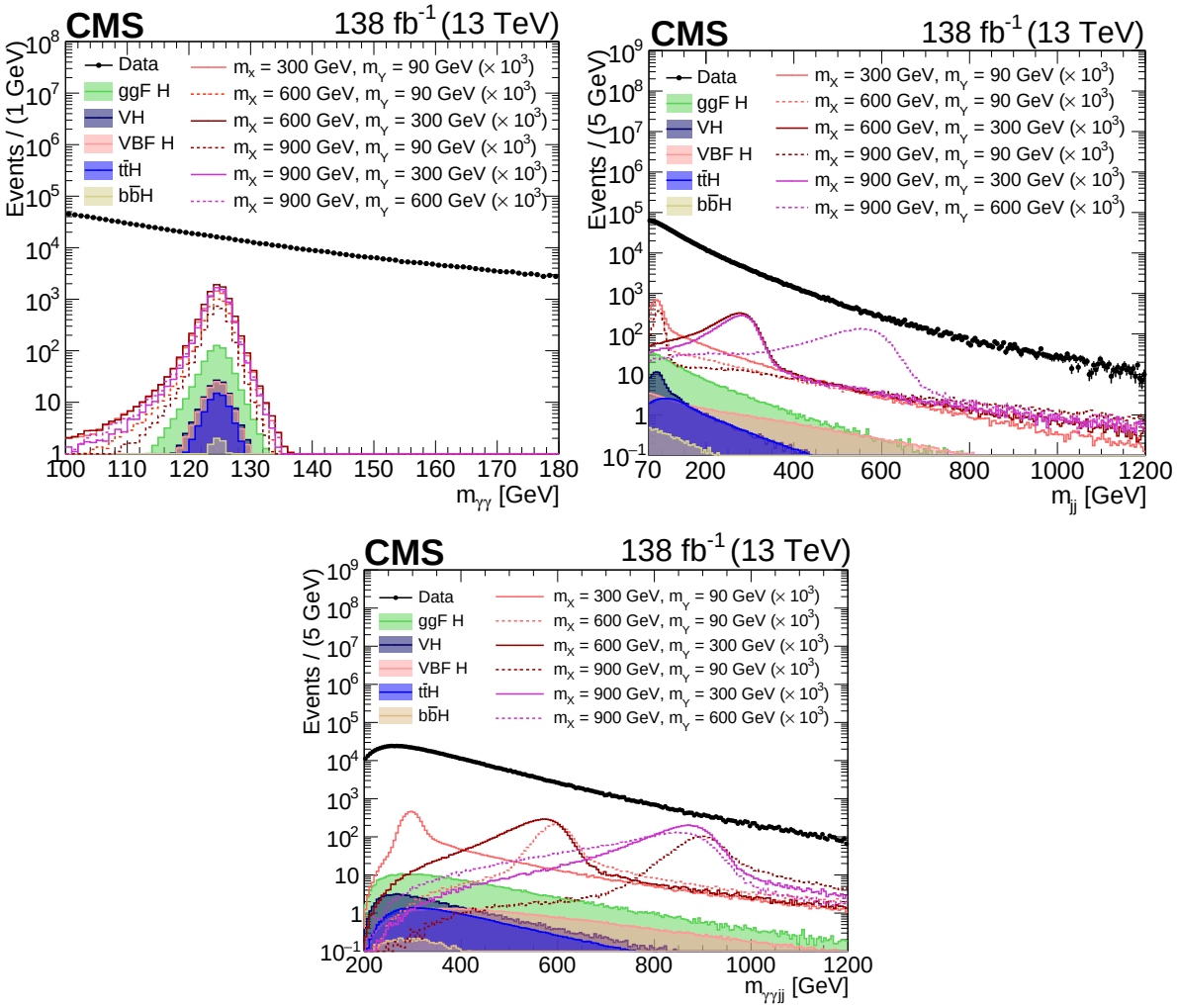

Figure 2: The $m_{\gamma\gamma}$ (upper left), m_{jj} (upper right) and $m_{\gamma\gamma jj}$ (lower) distributions in data and MC simulations. The signal distributions, shown for different values of m_X and m_Y with an assumption of 1 fb cross section, have been scaled up by a factor of 10^3.

4.2 Nonresonant background separation

The dominant nonresonant backgrounds stem from the SM multijet processes with up to two prompt photons. A boosted decision tree (BDT) discriminant is trained using MC simulations to separate signal and nonresonant backgrounds $\gamma\gamma$+jets and γ+jets. For this purpose, a gradient boosting algorithm, XGBOOST [75] is used to develop a multiclass BDT classifier.

Various resonant m_X and m_Y hypotheses with different kinematic distributions are studied within the analysis. The phase space is subdivided into three regions for m_X (< 500, 500–700, and > 700 GeV) and for m_Y (< 300, 300–500, and > 500 GeV). These ranges are combined into nine m_X–m_Y domains, three of which are forbidden by the energy conservation constraint $m_Y < m_X - m_H$. The mass ranges are decided according to the kinematic properties and Lorentz-boost factor, estimated by the quantity $m_X/(m_H + m_Y)$ [76], which defines similar angular properties. One BDT is trained per m_X–m_Y region. For each mass range in m_Y, a dedicated m_{jj} interval is defined: 70–400, 150–560, and 300–1000 GeV, respectively. Each interval is optimized to have the complete m_{jj} shape of the signals lying within one mass range to use as input for signal extraction.

For the purpose of BDT training, all simulated $X \to HY$ signal events that fit into a domain are combined into one sample with equal weights to build the signal sample. The simulated nonresonant background events are used as background samples, weighted by the products of their cross sections and the integrated luminosity. Before the training, the signal and background samples are normalized to unity. For HH searches, the training with m_{jj} interval 70–400 GeV is used since it already covers the m_{jj} interval of 70–190 GeV.

The signal and background events are intermixed and divided into train and test sets independently for every training. The input hyperparameters of the training are optimized using the 5-fold cross-validation [77] to mitigate over-training. An early-stopping feature of XGBOOST is also used to control the over-training. The BDT is trained for the three data-taking years together. The training strategy is validated by comparing the per year performance from the merged training with the performance obtained by the separate training for each year. The BDT training input variables, based on the two photons and two jets associated with the X decay, are motivated by Ref. [29]. They are grouped as follows:

1. Discriminating kinematic variables:
   - Helicity angles ($|\cos\theta^{CS}_{HY}|$, $|\cos\theta_{jj}|$, $|\cos\theta_{\gamma\gamma}|$), here CS refers to the Collins-Soper frame [78].
   - Minimum angular distances between photons and jets ($\Delta R_{\gamma j}$).
   - $p_T(jj)/m_{\gamma\gamma jj}$ and $p_T(\gamma\gamma)/m_{\gamma\gamma jj}$.
   - $p_T(\gamma)/m_{\gamma\gamma}$ and $p_T(j)/m_{jj}$ for leading and subleading photons and jets, respectively.
2. Object identification variables:
   - Leading- and subleading-p_T photon ID discriminant to reject misidentified photon contribution
   - Leading- and subleading-p_T jet b tagging discriminant to reject light jets
3. Resolution estimators:
   - Leading- and subleading-p_T photons: Energy resolution (σ_E/E) and mass resolution ($\sigma_{m_{\gamma\gamma}}/m_{\gamma\gamma}$);

- Leading- and subleading-p_T jets: p_T resolution ($\sigma_{p_T(j)}/p_T(j)$) and mass resolution ($\sigma_{m_{jj}}/m_{jj}$).

In addition to this, the transverse momentum deposits per unit area of the η–ϕ plane coming from pileup of the event, also known as the pileup transverse momentum density, is added in the inputs of the training to include pileup information which is different in the data-taking periods 2016–2018. The final BDT training output discriminates the signal from the background events by populating the signal events towards high BDT score and background events towards low BDT score. To preserve the signal statistics when defining optimal signal-enriched regions, the BDT outputs are transformed, ensuring that the combined signal BDT output distribution in each m_X–m_Y domain becomes uniform. It should be noted that, for a given value of m_X and m_Y, the BDT distribution may exhibit some departure from flatness, especially at very high BDT scores. We have verified for all signal hypotheses that this transformation, made for convenience, does not affect the analysis performance. The distribution of one of the BDT outputs for data and simulated events is shown in Fig. 3.

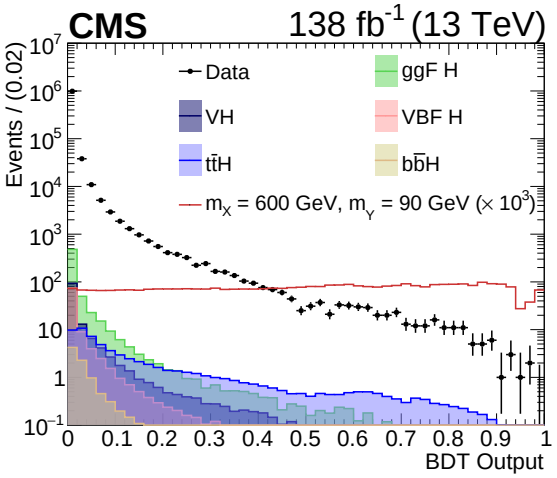

Figure 3: The distribution of the BDT output in data and MC simulations of the single H background processes and a signal, in m_X = 500–700 GeV and $m_Y < 300$ GeV range. The signal distribution, with an assumption of 1 fb cross section, has been scaled up by a factor of 10^3.

4.3 Event classification

We classify events into three categories based on BDT output along with a selection on $\widetilde{M}_X$. The optimization of the BDT categories and $\widetilde{M}_X$ selection is performed independently aiming for the best signal sensitivity using only the simulations.

The categorization remains the same for the signals within an m_X–m_Y domain. A constraint is imposed on the background statistics, requiring a minimum of 10 events within each category during the optimization of BDT boundaries. This minimum number of events in category optimization is chosen so that the systematic uncertainties from the background modeling do not exceed the benefits of a better signal over background ratio. Notably, this constraint excludes events falling within the $m_{\gamma\gamma} = [115, 135]$ GeV region. This approach ensures a sufficient number of background events in the $m_{\gamma\gamma}$ side-bands for each category, to guarantee a robust background modeling. We use signal and nonresonant background simulations to define categories based on the Punzi figure of merit [79] defined as $\epsilon_s/(1+\sqrt{B})$, where ϵ_s is signal efficiency and B refers to background yield. The category optimization remains independent of assuming any signal cross section since the figure of merit only uses signal efficiency, which prevents

Table 2: The BDT based event classification according to defined m_X (and m_Y) ranges for HH (and HY) searches. For HH searches, the column with $m_Y < 300\,\text{GeV}$ is used. The number represents the BDT scores showing a decreasing signal purity region from category 0 to 2.

	$m_Y < 300\,\text{GeV}$	$m_Y = [300\text{–}500]\,\text{GeV}$	$m_Y > 500\,\text{GeV}$
$m_X < 500\,\text{GeV}$	CAT 0 = 0.63–1.0 CAT 1 = 0.33–0.63 CAT 2 = 0.17–0.33		
$m_X = [500\text{–}700]\,\text{GeV}$	CAT 0 = 0.55–1.0 CAT 1 = 0.40–0.55 CAT 2 = 0.21–0.40	CAT 0 = 0.60–1.0 CAT 1 = 0.35–0.60 CAT 2 = 0.18–0.35	
$m_X > 700\,\text{GeV}$	CAT 0 = 0.50–1.0 CAT 1 = 0.30–0.50 CAT 2 = 0.21–0.30	CAT 0 = 0.35–1.0 CAT 1 = 0.24–0.35 CAT 2 = 0.18–0.24	CAT 0 = 0.40–1.0 CAT 1 = 0.29–0.40 CAT 2 = 0.13–0.29

categorization bias towards any specific signal hypothesis. The categories for different m_X–m_Y domains are shown in Table 2. The categories are labeled with 0 to 2 from the highest to lowest purity. For HH searches, categorization in $m_Y < 300\,\text{GeV}$ region is used. The signal efficiency gets reduced by up to a factor of 2 after BDT categorization.

The $\widetilde{M}_X$ selection differs depending upon m_X. For the HH analysis, a selection on $\widetilde{M}_X$ retaining at least 60% of the selected signal events is defined separately for each m_X hypothesis as shown in Fig. 4. This selection remains the same for HH and HY signals because, for low m_Y, the $\widetilde{M}_X$-resolution of HY signals is similar to HH signals. In contrast, for high m_Y, $\widetilde{M}_X$ holds better resolution, giving higher signal efficiency with the same selection.

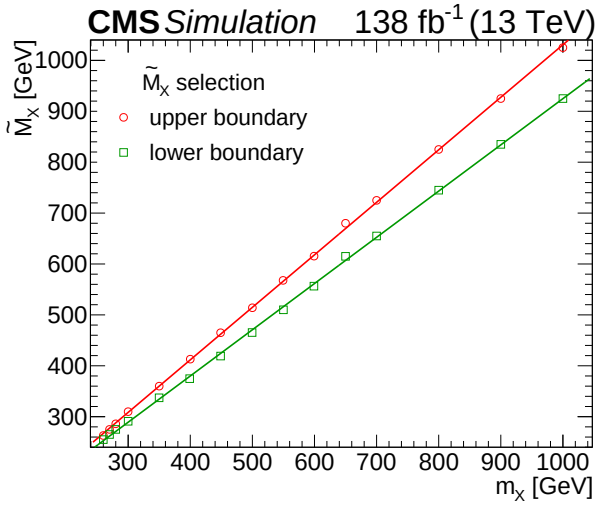

Figure 4: $\widetilde{M}_X$ selection for each m_X in HH and HY signals. The red and green lines represent the upper and lower boundary of this selection.

4.4 Resonant background rejection

The resonant backgrounds originate from the production of single H. Their contribution is strongly reduced by a tight selection applied on the $\widetilde{M}_X$ for each m_X hypothesis as stated in

Section 4.3. Nevertheless, for $m_X < 550\,\text{GeV}$, the presence of $t\bar{t}H$, containing genuine b jets from top quark decays, remains significant. A DNN-based discriminant was developed to further reduce it for the nonresonant $HH \to \gamma\gamma b\bar{b}$ analysis [29]. Using the same working points for the DNN as in Ref. [29] improved the limits by up to 10%. For $m_X > 550\,\text{GeV}$, the single H contribution in the total background is negligible, therefore, no selection on the discriminant is applied. Also, it is checked using the MC simulations that this selection does not distort the background mass distributions.

4.5 Signal and background modeling

For signal extraction, simultaneous fits are conducted on the $m_{\gamma\gamma}$ and m_{jj} distributions. Initially, separate parametric fits are executed for each category on these distributions. Subsequently, the final signal and background models are constructed by taking the product of the independent $m_{\gamma\gamma}$ and m_{jj} models. This independence was verified for signal, background simulations, and data by studying the possible correlations using the 2D distributions of the $m_{\gamma\gamma}$ and m_{jj} observables which were found to be negligible [29]. For signal and resonant backgrounds, MC simulations are used for $m_{\gamma\gamma}$ and m_{jj} modeling, while the $m_{\gamma\gamma}$ and m_{jj} distributions in data are used to choose optimal analytical background model. The $m_{\gamma\gamma}$ fit range remains same for all the signal and background models. The m_{jj} fit range differs depending upon the signal hypothesis. The following m_{jj} fit ranges are used: 70–190 GeV in HH searches and for $m_Y \leq 150\,\text{GeV}$ in HY searches; 70–400 GeV for $m_Y \in (150, 300)\,\text{GeV}$; 150–560 GeV for $m_Y \in [300, 500]\,\text{GeV}$; 300–1000 GeV for $m_Y > 500\,\text{GeV}$. During the final fit procedure, the shape parameters are allowed to float within the statistical constraints provided by the MC events used to build them.

For signal modeling, categorized events are fitted with a product of two parametric signal models: A sum of Gaussian distributions for $m_{\gamma\gamma}$ and a double-sided Crystal Ball (CB) function [80] or the sum of a CB and a Gaussian function for m_{jj}. The $m_{\gamma\gamma}$ distribution is parametrized using the sum of up to five Gaussian functions without any constraint to have a common mean.

To model the resonant single H backgrounds, the $m_{\gamma\gamma}$ distribution is constructed from the MC simulations following the same methodology used for the signal $m_{\gamma\gamma}$ model. The m_{jj} modeling depends on the production mechanism of the single H process, and a parameterization is obtained from the simulated distributions: for the ggF H and VBF H processes, the m_{jj} distribution is modeled with a Bernstein polynomial; for VH production, a CB function is used to model the distribution of the hadronic decays of vector bosons; for $t\bar{t}H$, where the two b jets are produced from a top quark decay, a Gaussian function with a mean value of 120 GeV is used. These backgrounds are negligible for $m_X > 550\,\text{GeV}$, therefore, they are absorbed within the nonresonant background model coming from data to simplify the signal extraction procedure.

The nonresonant background model is extracted from data using the discrete profiling method described in Refs. [68, 81]. This method makes use of polynomial and exponential functions to decide the analytic functions to fit the background $m_{\gamma\gamma}$ and m_{jj} distributions. It estimates the systematic uncertainty associated with these functions and treats the choice of background function as a discrete nuisance parameter in the likelihood fit to the data. For background modeling, the fit functions are optimized on data where the events from the signal region with $115 < m_{\gamma\gamma} < 135\,\text{GeV}$ are not taken into account. Considering the negligible correlation between $m_{\gamma\gamma}$ and m_{jj}, a set of MC pseudo-experiments were generated with and without injecting fake signal and fitted using the factorized 2D model. Negligible bias, as defined in Ref. [2], has been found which validates the robustness of the background model [82].

5 Systematic uncertainties

The impact of several sources of systematic uncertainties is considered in the analysis. The nonresonant background model is constructed using a data-driven method, and the uncertainties associated with the choice of background fit function are taken into account by the discrete profiling method described in Section 4.5. The systematic uncertainties can affect both the shapes and the normalizations of the $m_{\gamma\gamma}$ and m_{jj} distributions of the signal and the resonant single H backgrounds. Systematic uncertainties modifying the shape of the $m_{\gamma\gamma}$ and m_{jj} distributions are built into the models as parametric nuisance parameters.

The theoretical and experimental systematic uncertainties described below impact the normalization of the signal and single H backgrounds. The uncertainties in the cross sections arising from the quantum chromodynamics (QCD) renormalization and factorization scale variations, and PDF uncertainties are considered only for the single H processes. The uncertainties in the branching fractions of the H decay are considered for both the single H backgrounds and signals. Among these, the uncertainty from the QCD scale variations is the dominant one. The uncertainty is computed by varying both scales independently up and down by a factor of 2, while disregarding the two extreme combinations of variation. The theoretical uncertainties are treated as fully correlated across the three data-taking years.

The experimental uncertainties modifying the normalization are studied separately for each category, and they are mostly treated as uncorrelated across the different data-taking years. The dominant sources among them are:

- *Jet energy scale and resolution corrections*: These are measured using the method of balancing of jet p_T in dijet, γ+jet, Z+jet, and multijet events [44, 83]. The uncertainties in these corrections vary from 1–2% depending upon the p_T and η of jets. Their impact on the normalization is evaluated by varying the corrections within their uncertainties and propagating them to the final result.
- *Jet b tagging*: The DEEPJET discriminator distributions in MC simulations are reshaped by data-to-simulation scale factors [71]. The impact from different systematic uncertainty sources on the reshaping is studied. The highest impact comes from the misidentification of light flavor jets as b jets. The average magnitude of the uncertainty in b tagging efficiency varies from 4–6%.
- *Integrated luminosity*: The integrated luminosities for the 2016, 2017, and 2018 data-taking years have individual uncertainties of 1.2–2.5% [47–49], while the overall uncertainty in the measurement for the 2016–2018 period is 1.6%. The possible correlations from different common sources of luminosity measurements are taken into account.
- *Trigger efficiency*: This efficiency is calculated with the "tag-and-probe" method using $Z \to ee$ events [84]. The average size of uncertainty in the efficiency is 1–2% and the impact on the limits is less than 1%. An additional uncertainty is also added to include the trigger inefficiency arising from a gradual shift in the timing of the inputs of the ECAL L1 trigger for $|\eta| > 2.0$ in 2016–2017 data-taking years [33]. However, it does not impact the results.
- *Photon preselection uncertainty*: The efficiency after photon preselections is measured in simulations and data on $Z \to ee$ events using the "tag-and-probe" method [84]. The ratio of the efficiencies from data and MC simulations is used to derive the correction factor and corresponding uncertainties. Overall, it has an impact of less than 1% on the limits.

- *Photon energy scale and resolution*: These uncertainties associated with the corrections are estimated using $Z \to ee$ events and applied to data for the scale corrections and to MC simulations for resolution corrections [39]. The average size of uncertainty is 1–2% with less than 1% impact on the limits.

The impact of other sources of systematic uncertainty is small. The impact of the total systematic uncertainty on the limits for the $m_X < 500\,\text{GeV}$ and $m_Y < 250\,\text{GeV}$ is 1–2%. For other mass ranges, this impact is less than 1%. The dominant experimental systematic uncertainty is associated with the b tagging scale factors.

6 Results

A likelihood function is defined using signal and background analytic models of $m_{\gamma\gamma}$ and m_{jj} distributions, optimized as described in Section 4.5, with nuisance parameters related to the uncertainties explained in Section 5. A simultaneous unbinned 2D maximum likelihood fit to the $m_{\gamma\gamma}$ and m_{jj} distributions is performed on three event categories to extract the signal. Figure 5 shows the data and signal-plus-background fit for $m_{\gamma\gamma}$ and m_{jj} observables in CAT 0 defined in Table 2 and with $\widetilde{M}_X$ selection for two signal hypotheses from HH and HY searches. For HH searches, no statistically significant deviations in data are observed with respect to the background-only hypothesis. For HY searches, $m_{\gamma\gamma}$ and m_{jj} distributions in data are shown in the lower panel of Fig. 5 for the signal hypothesis where the largest excess is observed for m_X = 650 GeV and m_Y = 90 GeV with a local significance of $3.8\,\sigma$.

In order to account for the "Look elsewhere effect" [85], a global significance is calculated in the partial phase space of m_X within the range 300–1000 GeV and m_Y within the range 90–150 GeV, which amounts to $2.8\,\sigma$, with a corresponding p-value of 0.0027. This partial phase space is sufficient to provide an *upper limit* of the global significance, the true value of which would be lower if the full phase space is used. In other words, the chosen phase space is sufficient to demonstrate that the excess is not globally significant.

The observed excess being not statistically significant, we set upper limits at 95% confidence level (CL) on the product of resonant production cross section and branching fraction to $\gamma\gamma b\bar{b}$ channel using the CL_s criterion [86], taking the LHC profile likelihood ratio as a test statistic [87]. The asymptotic approximation is used in the limit setting procedure [86, 88, 89].

Figure 6 shows the upper limits on resonant production cross section as a function of resonance mass m_X for HH searches. The expected limits decrease from low to high m_X region and observed limits are consistent with them within ± 2 standard deviations ($\pm 2\,\sigma$). Depending on m_X, the observed upper limits at 95% CL vary between 0.82–0.07 and 0.78–0.06 fb for spin-0 and -2 resonant HH searches, respectively. The corresponding expected ranges are 0.74–0.08 and 0.65–0.06 fb, respectively. Following the theoretical cross sections from Ref. [18], these results exclude masses up to 600 GeV for spin-0 bulk radion signal at $\Lambda_R = 6\,\text{TeV}$ and up to 850 GeV for spin-2 bulk KK graviton signal with coupling factor of $\kappa/\overline{M}_{pl} = 0.5$.

Figure 7 describes the upper limits at 95% CL for the $pp \to X \to HY \to \gamma\gamma b\bar{b}$ signal as a function of m_Y with different m_X hypotheses. For every value of m_X, the expected limits first improve and then worsen with increasing m_Y. Indeed, when m_Y increases, the signal boost factor decreases, which leads to a drop in the signal selection efficiency. The observed limits remain consistent with the expected limits within $\pm 2\,\sigma$ of deviation, except for m_X = 650 GeV and $m_Y \leq 100\,\text{GeV}$. The observed and expected limits vary between 0.90–0.04 and 0.79–0.05 fb depending upon the mass ranges in m_X and m_Y, respectively.

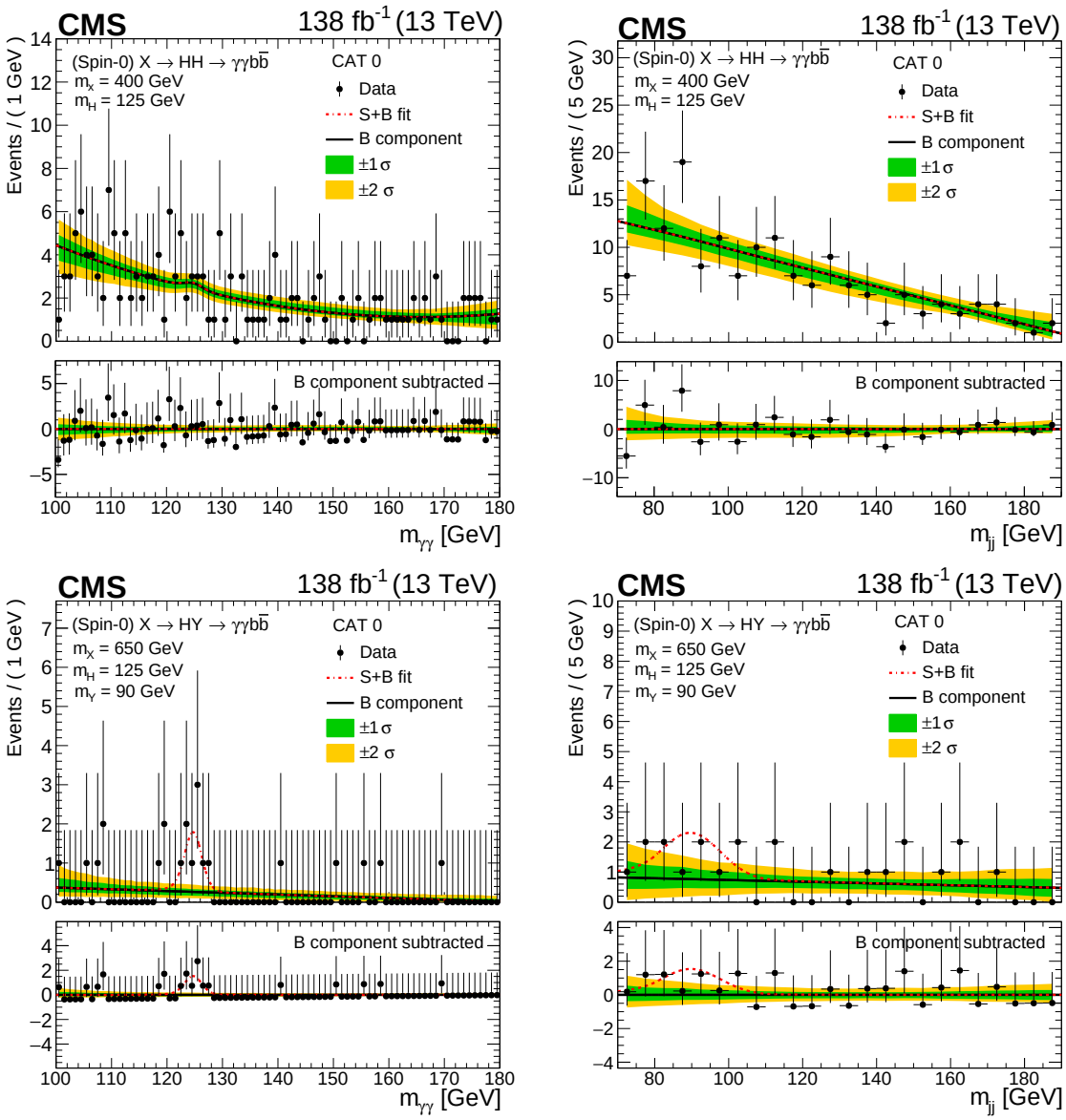

Figure 5: Invariant mass distributions $m_{\gamma\gamma}$ (left) and m_{jj} (right) with the data events (black markers), with $\widetilde{M}_X$ selection corresponding to an HH signal with $m_X = 400\,\text{GeV}$ (upper panel), and to an HY signal with $m_X = 650\,\text{GeV}$ and $m_Y = 90\,\text{GeV}$ (lower panel). The distributions are shown for the high signal purity category (CAT 0). The red dashed line shows the sum of the fitted signal and background events. The solid black line represents the total background component, including nonresonant and resonant background events. The green and yellow bands represent the ±1- and ±2-standard deviations which include the uncertainties in fit to the background-only hypothesis. The lower panel in each plot shows the residual signal yield after the background subtraction.

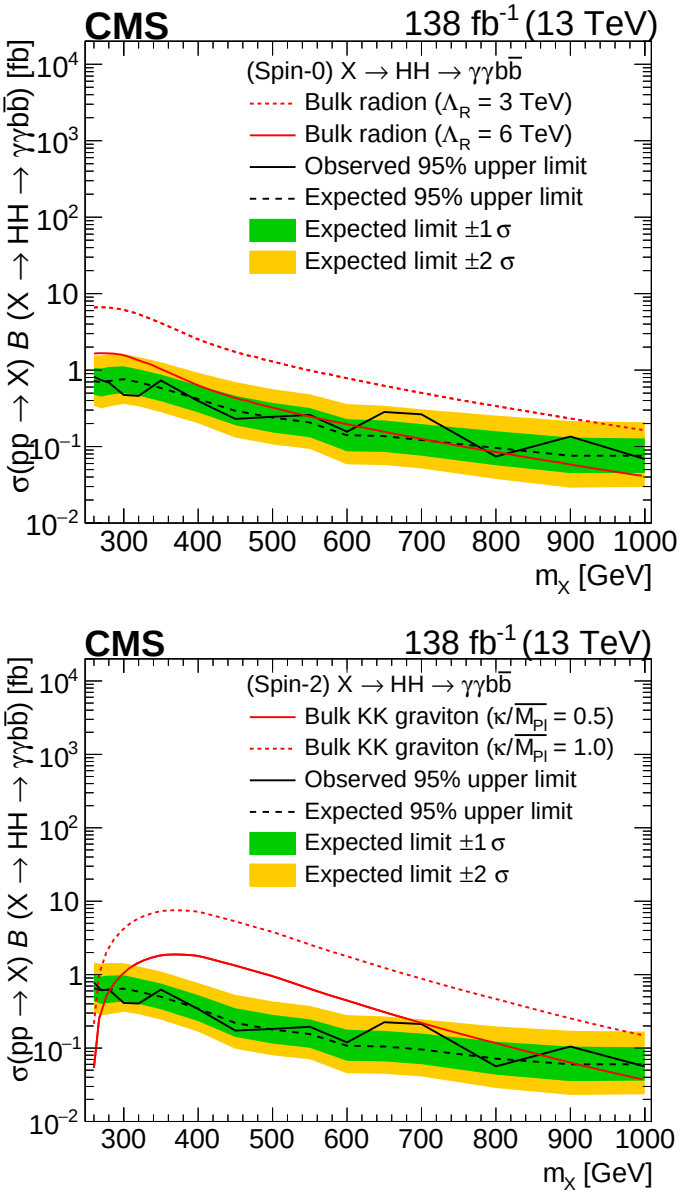

Figure 6: Expected and observed 95% CL upper limit on the product of resonant production cross section and branching fraction for spin-0 (upper) and spin-2 (lower) $pp \to X \to HH \to \gamma\gamma b\bar{b}$ signal hypotheses. The dashed and solid black lines represent expected and observed limits, respectively. The green and yellow bands represent the ± 1 and ± 2 standard deviations for the expected limit. The red lines show the theoretical predictions with different energy scales and couplings.

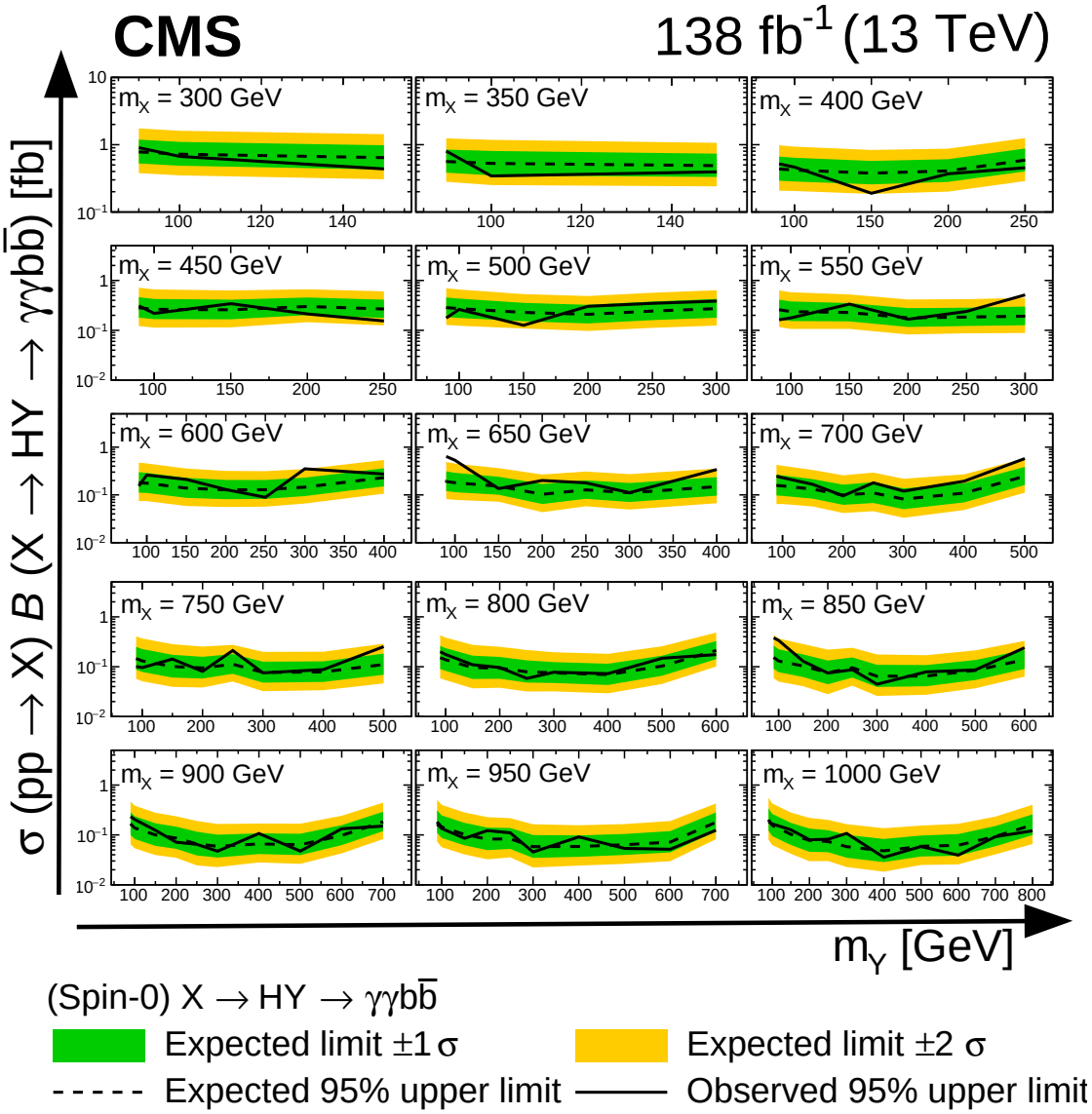

Figure 7: Expected and observed 95% CL exclusion limit on production cross section for $pp \to X \to HY \to \gamma\gamma b\bar{b}$ signal. The dashed and solid black lines represent expected and observed limits, respectively. The green and yellow bands represent the ± 1 and ± 2 standard deviations for the expected limit. The middle plot in the 3rd row shows the largest excess observed for m_X = 650 GeV and m_Y = 90 GeV.

This search loses its sensitivity above the specified m_X range since the $b\bar{b}b\bar{b}$ final state becomes more sensitive for HH searches, taking advantage of its larger branching fraction [90]. With the improved object identification methods and analysis strategy, the search shows up to 25% improvement on the HH limits when performed with 2016 data only in comparison to the ones previously published by the CMS Collaboration [28]. This search reports best-to-date limits for the HH searches in the region with $m_X < 800\,\text{GeV}$. Furthermore, the observed (expected) limits are better than those reported by the ATLAS Collaboration for HH searches in the $\gamma\gamma b\bar{b}$ channel using the 2016–2018 data by up to 40% (30%) [91]. For HY searches, this is the first result in the $\gamma\gamma b\bar{b}$ final state, where the analysis reports the best-to-date sensitivity within the m_X range of 300–1000 GeV and the m_Y range of 200–800 GeV.

The best-fit value of the product of the cross section with the branching fraction for the decay into $\gamma\gamma b\bar{b}$ at the largest excess is $\sigma(pp \to X \to HY \to \gamma\gamma b\bar{b}) = (0.35 \pm {}^{0.17}_{0.13})\,\text{fb}$. Given that no additional treatment is applied to the single H backgrounds for $m_X > 550\,\text{GeV}$ and they are assumed to be included within the nonresonant background model extracted from data due to their minimal contribution (see Section 4.4 and 4.5), a study was conducted to examine the impact of this simplification of the background modeling on the observed local excess. The study involves quantifying resonant and nonresonant background models separately as a part of the final background model. The results indicate a reduction in the local significance of 8% in units of standard deviation, and 6% in the best-fit value of the cross section. This effect is well within the bias range accepted in this analysis following the Ref. [2].

Figure 8 compares the expected and observed upper limits to the product of the theoretical signal production cross section and the branching fraction $pp \to X \to HY \to \gamma\gamma b\bar{b}$. The theoretical predictions are defined as the maximally allowed cross sections for a given m_X and m_Y hypothesis within the NMSSM framework [92]. It is provided by the LHC Higgs Working Group and derived from the codes NMSSMTOOLS 5.5.0 [93] and NMSSMCALC [94]. The predictions integrate constraints from measurements of H properties, SUSY searches, B-meson physics, and dark matter searches. For this model, both expected and observed limits are below the theoretical cross sections for some of the signal hypotheses, leading to the exclusion of masses between 400–650 GeV in m_X and 90–300 GeV in m_Y.

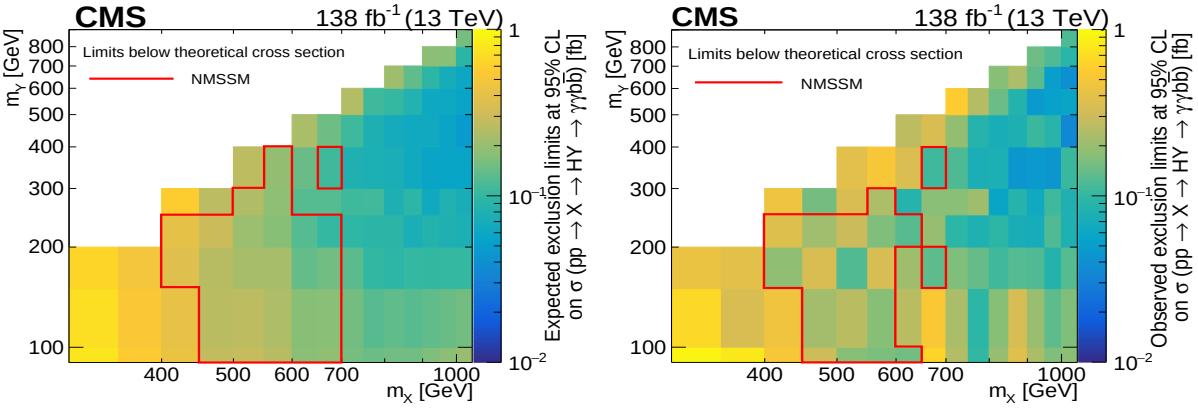

Figure 8: Comparison of the expected (left) and observed (right) limits at 95% CL with the maximally allowed cross sections from the NMSSM model where the area within the red contours indicate the excluded mass regions. The limits are displayed as two-dimensional binned distributions.

7 Summary

A search for a new resonance X, decaying either to a pair of Higgs bosons HH or to an H and a new spin-0 boson Y, is presented. The search uses data from proton-proton collisions collected by the CMS experiment at the Large Hadron Collider in 2016–2018 at a center-of-mass energy of 13 TeV, corresponding to 138 fb^{-1} of integrated luminosity. The search targets beyond standard model particles as predicted by several models of new physics. For X decaying to HH, an m_X range of 260–1000 GeV is covered, while for X decaying to HY, the search range is 300–1000 GeV in m_X and 90–800 GeV in m_Y. Results are presented as the upper limits at 95% confidence level on the product of the production cross section of X and its branching fraction to the $\gamma\gamma\text{b}\bar{\text{b}}$ final state, through either HH or HY decays. Depending upon the mass range, the observed limits for a spin-0 resonance X decaying to HH range from 0.82–0.07 fb, while the expected limits are 0.74–0.08 fb. For X decaying to HY, the observed limits are 0.90–0.04 fb, while the expected limits lie in the range 0.79–0.05 fb, depending on the masses m_X and m_Y. The data are found to be compatible with the standard model predictions over the searched domains. The largest deviation from the background-only hypothesis, with a local significance of 3.8 standard deviations, is observed for m_X = 650 GeV and m_Y =90 GeV. However, this excess is not considered significant as it is reduced to 2.8 standard deviations when a partial look-elsewhere effect is considered. The HY search is performed for the first time in the $\gamma\gamma\text{b}\bar{\text{b}}$ channel. The limits from the HH search are the most stringent to date for m_X less than 800 GeV.

Acknowledgments

We congratulate our colleagues in the CERN accelerator departments for the excellent performance of the LHC and thank the technical and administrative staffs at CERN and at other CMS institutes for their contributions to the success of the CMS effort. In addition, we gratefully acknowledge the computing centers and personnel of the Worldwide LHC Computing Grid and other centers for delivering so effectively the computing infrastructure essential to our analyses. Finally, we acknowledge the enduring support for the construction and operation of the LHC, the CMS detector, and the supporting computing infrastructure provided by the following funding agencies: SC (Armenia), BMBWF and FWF (Austria); FNRS and FWO (Belgium); CNPq, CAPES, FAPERJ, FAPERGS, and FAPESP (Brazil); MES and BNSF (Bulgaria); CERN; CAS, MoST, and NSFC (China); MINCIENCIAS (Colombia); MSES and CSF (Croatia); RIF (Cyprus); SENESCYT (Ecuador); MoER, ERC PUT and ERDF (Estonia); Academy of Finland, MEC, and HIP (Finland); CEA and CNRS/IN2P3 (France); SRNSF (Georgia); BMBF, DFG, and HGF (Germany); GSRI (Greece); NKFIH (Hungary); DAE and DST (India); IPM (Iran); SFI (Ireland); INFN (Italy); MSIP and NRF (Republic of Korea); MES (Latvia); LAS (Lithuania); MOE and UM (Malaysia); BUAP, CINVESTAV, CONACYT, LNS, SEP, and UASLP-FAI (Mexico); MOS (Montenegro); MBIE (New Zealand); PAEC (Pakistan); MES and NSC (Poland); FCT (Portugal); MESTD (Serbia); MCIN/AEI and PCTI (Spain); MOSTR (Sri Lanka); Swiss Funding Agencies (Switzerland); MST (Taipei); MHESI and NSTDA (Thailand); TUBITAK and TENMAK (Turkey); NASU (Ukraine); STFC (United Kingdom); DOE and NSF (USA).

Individuals have received support from the Indo-French Network in High Energy Physics financed by the Indo-French Center for the Promotion of Advanced Research-CEFIPRA; the Marie-Curie program and the European Research Council and Horizon 2020 Grant, contract Nos. 675440, 724704, 752730, 758316, 765710, 824093, and COST Action CA16108 (European Union); the Leventis Foundation; the Alfred P. Sloan Foundation; the Alexander von Humboldt Foundation; the Science Committee, project no. 22rl-037 (Armenia); the Belgian Federal Science Policy Office; the Fonds pour la Formation à la Recherche dans l'Industrie et dans

l'Agriculture (FRIA-Belgium); the Agentschap voor Innovatie door Wetenschap en Technologie (IWT-Belgium); the F.R.S.-FNRS and FWO (Belgium) under the "Excellence of Science – EOS" – be.h project n. 30820817; the Beijing Municipal Science & Technology Commission, No. Z191100007219010 and Fundamental Research Funds for the Central Universities (China); the Ministry of Education, Youth and Sports (MEYS) of the Czech Republic; the Shota Rustaveli National Science Foundation, grant FR-22-985 (Georgia); the Deutsche Forschungsgemeinschaft (DFG), under Germany's Excellence Strategy – EXC 2121 "Quantum Universe" – 390833306, and under project number 400140256 - GRK2497; the Hellenic Foundation for Research and Innovation (HFRI), Project Number 2288 (Greece); the Hungarian Academy of Sciences, the New National Excellence Program - ÚNKP, the NKFIH research grants K 124845, K 124850, K 128713, K 128786, K 129058, K 131991, K 133046, K 138136, K 143460, K 143477, 2020-2.2.1-ED-2021-00181, and TKP2021-NKTA-64 (Hungary); the Council of Science and Industrial Research, India; the Latvian Council of Science; the Ministry of Education and Science, project no. 2022/WK/14, and the National Science Center, contracts Opus 2021/41/B/ST2/01369 and 2021/43/B/ST2/01552 (Poland); the Fundação para a Ciência e a Tecnologia, grant CEECIND/01334/2018 (Portugal); the National Priorities Research Program by Qatar National Research Fund; MCIN/AEI/10.13039/501100011033, ERDF "a way of making Europe", and the Programa Estatal de Fomento de la Investigación Científica y Técnica de Excelencia María de Maeztu, grant MDM-2017-0765 and Programa Severo Ochoa del Principado de Asturias (Spain); the Chulalongkorn Academic into Its 2nd Century Project Advancement Project, and the National Science, Research and Innovation Fund via the Program Management Unit for Human Resources & Institutional Development, Research and Innovation, grant B05F650021 (Thailand); the Kavli Foundation; the Nvidia Corporation; the SuperMicro Corporation; the Welch Foundation, contract C-1845; and the Weston Havens Foundation (USA).

References

[1] ATLAS Collaboration, "Observation of a new particle in the search for the standard model Higgs boson with the ATLAS detector at the LHC", *Phys. Lett. B* **716** (2012) 1, doi:10.1016/j.physletb.2012.08.020, arXiv:1207.7214.

[2] CMS Collaboration, "Observation of a new boson at a mass of 125 GeV with the CMS experiment at the LHC", *Phys. Lett. B* **716** (2012) 30, doi:10.1016/j.physletb.2012.08.021, arXiv:1207.7235.

[3] CMS Collaboration, "Observation of a new boson with mass near 125 GeV in pp collisions at $\sqrt{s}$ = 7 and 8 TeV", *JHEP* **06** (2013) 081, doi:10.1007/JHEP06(2013)081, arXiv:1303.4571.

[4] S. Weinberg, "A model of leptons", *Phys. Rev. Lett.* **19** (1967) 1264, doi:10.1103/PhysRevLett.19.1264.

[5] Sheldon L. Glashow, "Partial-symmetries of weak interactions", *Nucl. Phys.* **22** (1961) 579, doi:10.1016/0029-5582(61)90469-2.

[6] G. 't Hooft and M. Veltman, "Regularization and renormalization of gauge fields", *Nucl. Phys. B* **44** (1972) 189, doi:10.1016/0550-3213(72)90279-9.

[7] P. W. Higgs, "Broken symmetries, massless particles and gauge fields", *Phys. Lett.* **12** (1964) 132, doi:10.1016/0031-9163(64)91136-9.

[8] P. W. Higgs, "Broken symmetries and the masses of gauge bosons", *Phys. Rev. Lett.* **13** (1964) 508, doi:10.1103/PhysRevLett.13.508.

[9] CMS Collaboration, "A portrait of the Higgs boson by the CMS experiment ten years after the discovery", *Nature* **607** (2022) 60, doi:10.1038/s41586-022-04892-x, arXiv:2207.00043.

[10] L. Randall and R. Sundrum, "An Alternative to compactification", *Phys. Rev. Lett.* **83** (1999) 4690, doi:10.1103/PhysRevLett.83.4690, arXiv:hep-th/9906064.

[11] L. Randall and R. Sundrum, "Large mass hierarchy from a small extra dimension", *Phys. Rev. Lett.* **83** (1999) 3370, doi:10.1103/PhysRevLett.83.3370, arXiv:hep-ph/9905221.

[12] W. D. Goldberger and M. B. Wise, "Modulus stabilization with bulk fields", *Phys. Rev. Lett.* **83** (1999) 4922, doi:10.1103/PhysRevLett.83.4922, arXiv:hep-ph/9907447.

[13] C. Csáki, M. Graesser, L. Randall, and J. Terning, "Cosmology of brane models with radion stabilization", *Phys. Rev. D* **62** (2000) 045015, doi:10.1103/PhysRevD.62.045015, arXiv:hep-ph/9911406.

[14] C. Csáki, M. L. Graesser, and G. D. Kribs, "Radion dynamics and electroweak physics", *Phys. Rev. D* **63** (2001) 065002, doi:10.1103/PhysRevD.63.065002, arXiv:hep-th/0008151.

[15] H. Davoudiasl, J. L. Hewett, and T. G. Rizzo, "Phenomenology of the Randall–Sundrum Gauge Hierarchy Model", *Phys. Rev. Lett.* **84** (2000) 2080, doi:10.1103/PhysRevLett.84.2080, arXiv:hep-ph/9909255.

[16] O. DeWolfe, D. Z. Freedman, S. S. Gubser, and A. Karch, "Modeling the fifth dimension with scalars and gravity", *Phys. Rev. D* **62** (2000) 046008, doi:10.1103/PhysRevD.62.046008, arXiv:hep-th/9909134.

[17] K. Agashe, H. Davoudiasl, G. Perez, and A. Soni, "Warped gravitons at the CERN LHC and beyond", *Phys. Rev. D* **76** (2007) 036006, doi:10.1103/PhysRevD.76.036006, arXiv:hep-ph/0701186.

[18] A. Carvalho, "Gravity particles from Warped Extra Dimensions, predictions for LHC", 3, 2014. arXiv:1404.0102.

[19] Yu. A. Golfand and E. P. Likhtman, "Extension of the algebra of Poincaré group generators and violation of p invariance", *JETP Lett.* **13** (1971) 323, doi:10.1142/9789814542340_0001.

[20] J. Wess and B. Zumino, "Supergauge transformations in four-dimensions", *Nucl. Phys. B* **70** (1974) 39, doi:10.1016/0550-3213(74)90355-1.

[21] P. Fayet, "Supergauge invariant extension of the Higgs mechanism and a model for the electron and its neutrino", *Nucl. Phys. B* **90** (1975) 104, doi:10.1016/0550-3213(75)90636-7.

[22] P. Fayet, "Spontaneously broken supersymmetric theories of weak, electromagnetic and strong interactions", *Phys. Lett. B* **69** (1977) 489, doi:10.1016/0370-2693(77)90852-8.

[23] U. Ellwanger, C. Hugonie, and A. M. Teixeira, "The Next-to-Minimal Supersymmetric Standard Model", *Phys. Rept.* **496** (2010) 1, doi:10.1016/j.physrep.2010.07.001, arXiv:0910.1785.

[24] M. Maniatis, "The Next-to-Minimal Supersymmetric extension of the Standard Model reviewed", *Int. J. Mod. Phys. A* **25** (2010) 3505, doi:10.1142/S0217751X10049827, arXiv:0906.0777.

[25] J. E. Kim and H. P. Nilles, "The μ-problem and the strong CP problem", *Phys. Lett. B* **138** (1984) 150, doi:10.1016/0370-2693(84)91890-2.

[26] T. Robens, T. Stefaniak, and J. Wittbrodt, "Two-real-scalar-singlet extension of the SM: LHC phenomenology and benchmark scenarios", *Eur. Phys. J. C* **80** (2020) 151, doi:10.1140/epjc/s10052-020-7655-x, arXiv:1908.08554.

[27] D. de Florian et al., "Handbook of LHC Higgs cross sections: 4. Deciphering the nature of the Higgs sector", 2016. arXiv:1610.07922. CERN-2017-002-M.

[28] CMS Collaboration, "Search for Higgs boson pair production in the $\gamma\gamma b\bar{b}$ final state in pp collisions at $\sqrt{s} = 13$ TeV", *Phys. Lett. B* **788** (2019) 7, doi:10.1016/j.physletb.2018.10.056, arXiv:1806.00408.

[29] CMS Collaboration, "Search for nonresonant Higgs boson pair production in final states with two bottom quarks and two photons in proton-proton collisions at $\sqrt{s}$ = 13 TeV", *JHEP* **03** (2021) 257, doi:10.1007/JHEP03(2021)257, arXiv:2011.12373.

[30] HEPData record for this analysis, 2023. doi:10.17182/hepdata.142396.

[31] CMS Collaboration, "The CMS experiment at the CERN LHC", *JINST* **3** (2008) S08004, doi:10.1088/1748-0221/3/08/S08004.

[32] CMS Collaboration, "The CMS trigger system", *JINST* **12** (2017) P01020, doi:10.1088/1748-0221/12/01/P01020, arXiv:1609.02366.

[33] CMS Collaboration, "Performance of the CMS Level-1 trigger in proton-proton collisions at $\sqrt{s} = 13$ TeV", *JINST* **15** (2020) P10017, doi:10.1088/1748-0221/15/10/P10017, arXiv:2006.10165.

[34] CMS Collaboration, "The CMS high level trigger", *Eur. Phys. J. C* **46** (2006) 605, doi:10.1140/epjc/s2006-02495-8, arXiv:hep-ex/0512077.

[35] CMS Collaboration, "Particle-flow reconstruction and global event description with the CMS detector", *JINST* **12** (2017) P10003, doi:10.1088/1748-0221/12/10/P10003, arXiv:1706.04965.

[36] CMS Collaboration, "Measurements of Higgs boson properties in the diphoton decay channel in proton-proton collisions at $\sqrt{s} = 13$ TeV", *JHEP* **11** (2018) 185, doi:10.1007/JHEP11(2018)185, arXiv:1804.02716.

[37] E. Spyromitros-Xioufis, G. Tsoumakas, W. Groves, and I. Vlahavas, "Multi-target regression via input space expansion: treating targets as inputs", *Machine Learning* **104** (2016) 55, doi:10.1007/s10994-016-5546-z, arXiv:1211.6581.

[38] CMS Collaboration, "Electron and photon reconstruction and identification with the CMS experiment at the CERN LHC", *JINST* **16** (2021) P05014, doi:10.1088/1748-0221/16/05/P05014, arXiv:2012.06888.

[39] CMS Collaboration, "Performance of photon reconstruction and identification with the CMS detector in proton-proton collisions at $\sqrt{s} = 8$ TeV", *JINST* **10** (2015) P08010, doi:10.1088/1748-0221/10/08/P08010, arXiv:1502.02702.

[40] CMS Collaboration, "A measurement of the Higgs boson mass in the diphoton decay channel", *Phys. Lett. B* **805** (2020) 135425, doi:10.1016/j.physletb.2020.135425, arXiv:2002.06398.

[41] M. Cacciari, G. P. Salam, and G. Soyez, "The anti-k_T jet clustering algorithm", *JHEP* **04** (2008) 063, doi:10.1088/1126-6708/2008/04/063, arXiv:0802.1189.

[42] M. Cacciari, G. P. Salam, and G. Soyez, "FastJet user manual", *Eur. Phys. J. C* **72** (2012) 1896, doi:10.1140/epjc/s10052-012-1896-2, arXiv:1111.6097.

[43] M. Cacciari and G. P. Salam, "Pileup subtraction using jet areas", *Phys. Lett. B* **659** (2008) 119, doi:10.1016/j.physletb.2007.09.077, arXiv:0707.1378.

[44] CMS Collaboration, "Jet energy scale and resolution in the CMS experiment in pp collisions at 8 TeV", *JINST* **12** (2017) P02014, doi:10.1088/1748-0221/12/02/P02014, arXiv:1607.03663.

[45] CMS Collaboration, "A deep neural network for simultaneous estimation of b jet energy and resolution", *Comput. Softw. Big Sci.* **4** (2020) 10, doi:10.1007/s41781-020-00041-z, arXiv:1912.06046.

[46] CMS Collaboration, "Performance of missing transverse momentum reconstruction in proton-proton collisions at $\sqrt{s} = 13$ TeV using the CMS detector", *JINST* **14** (2019) P07004, doi:10.1088/1748-0221/14/07/P07004, arXiv:1903.06078.

[47] CMS Collaboration, "Precision luminosity measurement in proton-proton collisions at $\sqrt{s} = 13$ TeV in 2015 and 2016 at CMS", *Eur. Phys. J. C* **81** (2021) 800, doi:10.1140/epjc/s10052-021-09538-2, arXiv:2104.01927.

[48] CMS Collaboration, "CMS luminosity measurement for the 2017 data-taking period at $\sqrt{s}$ = 13 TeV", CMS Physics Analysis Summary CMS-PAS-LUM-17-004, 2018.

[49] CMS Collaboration, "CMS luminosity measurement for the 2018 data-taking period at $\sqrt{s} = 13$ TeV", CMS Physics Analysis Summary CMS-PAS-LUM-18-002, 2019.

[50] J. Alwall et al., "The automated computation of tree-level and next-to-leading order differential cross sections, and their matching to parton shower simulations", *JHEP* **07** (2014) 079, doi:10.1007/JHEP07(2014)079, arXiv:1405.0301.

[51] A. Alloul et al., "FeynRules 2.0 — A complete toolbox for tree-level phenomenology", *Comput. Phys. Commun.* **185** (2014) 2250, doi:10.1016/j.cpc.2014.04.012, arXiv:1310.1921.

[52] T. Gleisberg et al., "Event generation with SHERPA 1.1", *JHEP* **02** (2009) 007, doi:10.1088/1126-6708/2009/02/007, arXiv:0811.4622.

[53] T. Sjöstrand et al., "An introduction to PYTHIA 8.2", *Comput. Phys. Commun.* **191** (2015) 159, doi:10.1016/j.cpc.2015.01.024, arXiv:1410.3012.

[54] P. Nason, "A new method for combining NLO QCD with shower Monte Carlo algorithms", *JHEP* **11** (2004) 040, doi:10.1088/1126-6708/2004/11/040, arXiv:hep-ph/0409146.

[55] S. Frixione, P. Nason, and C. Oleari, "Matching NLO QCD computations with Parton Shower simulations: the POWHEG method", *JHEP* **11** (2007) 070, doi:10.1088/1126-6708/2007/11/070, arXiv:0709.2092.

[56] S. Alioli, P. Nason, C. Oleari, and E. Re, "A general framework for implementing NLO calculations in shower Monte Carlo programs: the POWHEG BOX", *JHEP* **06** (2010) 043, doi:10.1007/JHEP06(2010)043, arXiv:1002.2581.

[57] E. Bagnaschi, G. Degrassi, P. Slavich, and A. Vicini, "Higgs production via gluon fusion in the POWHEG approach in the SM and in the MSSM", *JHEP* **02** (2012) 088, doi:10.1007/JHEP02(2012)088, arXiv:1111.2854.

[58] M. Wiesemann et al., "Higgs production in association with bottom quarks", *JHEP* **02** (2015) doi:10.1007/jhep02(2015)132.

[59] CMS Collaboration, "Event generator tunes obtained from underlying event and multiparton scattering measurements", *Eur. Phys. J. C* **76** (2016) 155, doi:10.1140/epjc/s10052-016-3988-x, arXiv:1512.00815.

[60] CMS Collaboration, "Extraction and validation of a new set of CMS PYTHIA8 tunes from underlying-event measurements", *Eur. Phys. J. C* **80** (2020) 4, doi:10.1140/epjc/s10052-019-7499-4, arXiv:1903.12179.

[61] NNPDF Collaboration, "Parton distributions for the LHC Run II", *JHEP* **04** (2015) 040, doi:10.1007/JHEP04(2015)040, arXiv:1410.8849.

[62] NNPDF Collaboration, "Parton distributions from high-precision collider data", *Eur. Phys. J. C* **77** (2017) 663, doi:10.1140/epjc/s10052-017-5199-5, arXiv:1706.00428.

[63] S. Carrazza, J. I. Latorre, J. Rojo, and G. Watt, "A compression algorithm for the combination of PDF sets", *Eur. Phys. J. C* **75** (2015) 474, doi:10.1140/epjc/s10052-015-3703-3, arXiv:1504.06469.

[64] J. Butterworth et al., "PDF4LHC recommendations for LHC Run II", *J. Phys. G* **43** (2016) 023001, doi:10.1088/0954-3899/43/2/023001, arXiv:1510.03865.

[65] S. Dulat et al., "New parton distribution functions from a global analysis of quantum chromodynamics", *Phys. Rev. D* **93** (2016) 033006, doi:10.1103/PhysRevD.93.033006, arXiv:1506.07443.

[66] L. A. Harland-Lang, A. D. Martin, P. Motylinski, and R. S. Thorne, "Parton distributions in the LHC era: MMHT 2014 PDFs", *Eur. Phys. J. C* **75** (2015) 204, doi:10.1140/epjc/s10052-015-3397-6, arXiv:1412.3989.

[67] GEANT4 Collaboration, "GEANT4—a simulation toolkit", *Nucl. Instrum. Meth. A* **506** (2003) 250, doi:10.1016/S0168-9002(03)01368-8.

[68] CMS Collaboration, "Observation of the diphoton decay of the Higgs boson and measurement of its properties", *Eur. Phys. J. C* **74** (2014) 3076, doi:10.1140/epjc/s10052-014-3076-z, arXiv:1407.0558.

[69] CMS Collaboration, "Pileup mitigation at CMS in 13 TeV data", *JINST* **15** (2020) P09018, doi:10.1088/1748-0221/15/09/P09018, arXiv:2003.00503.

[70] B. Vormwald, "The CMS phase-1 pixel detector - experience and lessons learned from two years of operation", *JINST* **14** (2019) C07008, doi:10.1088/1748-0221/14/07/c07008.

[71] CMS Collaboration, "Identification of heavy-flavour jets with the CMS detector in pp collisions at 13 TeV", *JINST* **13** (2018) P05011, doi:10.1088/1748-0221/13/05/P05011, arXiv:1712.07158.

[72] E. Bols et al., "Jet Flavour Classification Using DeepJet", *JINST* **15** (2020) P12012, doi:10.1088/1748-0221/15/12/P12012, arXiv:2008.10519.

[73] CMS Collaboration, "Performance of the DeepJet b tagging algorithm using 41.9/fb of data from proton-proton collisions at 13 TeV with Phase 1 CMS detector", CMS Detector Performance Note CMS-DP-2018-058, 2018.

[74] N. Kumar and S. P. Martin, "LHC search for di-Higgs decays of stoponium and other scalars in events with two photons and two bottom jets", *Phys. Rev. D* **90** (2014) 055007, doi:10.1103/PhysRevD.90.055007, arXiv:1404.0996.

[75] T. Chen and C. Guestrin, "XGBoost: A scalable tree boosting system", in *Proceedings of the 22nd ACM SIGKDD International Conference on Knowledge Discovery and Data Mining*, KDD, p. 785. ACM, New York, NY, USA, 2016. doi:10.1145/2939672.2939785.

[76] M. Gouzevitch et al., "Scale-invariant resonance tagging in multijet events and new physics in Higgs pair production", *JHEP* **07** (2013) 148, doi:10.1007/JHEP07(2013)148, arXiv:1303.6636.

[77] T. Hastie, R. Tibshirani, and J. Friedman, "The elements of statistical learning". Springer-Verlag New York, 2nd edition, 2009. doi:10.1007/978-0-387-84858-7.

[78] J. C. Collins and D. E. Soper, "Angular distribution of dileptons in high-energy hadron collisions", *Phys. Rev. D* **16** (1977) 2219, doi:10.1103/PhysRevD.16.2219.

[79] G. Punzi, "Sensitivity of searches for new signals and its optimization", in *Statistical Problems in Particle Physics, Astrophysics, and Cosmology*, L. Lyons, R. Mount, and R. Reitmeyer, eds., p. 79. 2003. arXiv:physics/0308063.

[80] M. J. Oreglia, "A study of the reactions $\psi' \to \gamma\gamma\psi$". PhD thesis, Stanford University, 1980. SLAC Report SLAC-R-236.

[81] P. D. Dauncey, M. Kenzie, N. Wardle, and G. J. Davies, "Handling uncertainties in background shapes: the discrete profiling method", *JINST* **10** (2015) P04015, doi:10.1088/1748-0221/10/04/P04015, arXiv:1408.6865.

[82] D. L. Hahs-Vaughn and R. G. Lomax, "Statistical Concepts — A Second Course". Routledge New York, 4th edition, 2012. doi:10.4324/9780203137802.

[83] CMS Collaboration, "Jet algorithms performance in 13 TeV data", CMS Physics Analysis Summary CMS-PAS-JME-16-003, 2017.

[84] CMS Collaboration, "Measurement of the Inclusive W and Z Production Cross Sections in pp Collisions at $\sqrt{s} = 7$ TeV", *JHEP* **10** (2011) 132, doi:10.1007/JHEP10(2011)132, arXiv:1107.4789.

[85] E. Gross and O. Vitells, "Trial factors for the look elsewhere effect in high energy physics", *Eur. Phys. J. C* **70** (2010) 525, doi:10.1140/epjc/s10052-010-1470-8, arXiv:1005.1891.

[86] A. L. Read, "Presentation of search results: the CL_s technique", *J. Phys. G* **28** (2002) 2693, doi:10.1088/0954-3899/28/10/313.

[87] ATLAS and CMS Collaborations, LHC Higgs Combination Group, "Procedure for the LHC Higgs boson search combination in summer 2011", CMS/ATLAS joint note ATL-PHYS-PUB-2011-11, CMS NOTE 2011/005, 2011.

[88] T. Junk, "Confidence level computation for combining searches with small statistics", *Nucl. Instrum. Meth. A* **434** (1999) 435, doi:10.1016/S0168-9002(99)00498-2, arXiv:hep-ex/9902006.

[89] G. Cowan, K. Cranmer, E. Gross, and O. Vitells, "Asymptotic formulae for likelihood-based tests of new physics", *Eur. Phys. J. C* **71** (2011) 1554, doi:10.1140/epjc/s10052-011-1554-0, arXiv:1007.1727. [Erratum: doi:10.1140/epjc/s10052-013-2501-z].

[90] CMS Collaboration, "Combination of searches for Higgs boson pair production in proton-proton collisions at $\sqrt{s} = 13$ TeV", *Phys. Rev. Lett.* **122** (2019) 121803, doi:10.1103/PhysRevLett.122.121803, arXiv:1811.09689.

[91] ATLAS Collaboration, "Search for Higgs boson pair production in the two bottom quarks plus two photons final state in pp collisions at $\sqrt{s} = 13$ TeV with the ATLAS detector", *Phys. Rev. D* **106** (2022) 052001, doi:10.1103/PhysRevD.106.052001, arXiv:2112.11876.

[92] U. Ellwanger et al., "Benchmark lines and planes for Higgs-to-Higgs decays in the NMSSM", 3, 2024. arXiv:2403.15046.

[93] U. Ellwanger and C. Hugonie, "NMHDECAY 2.0: An Updated program for sparticle masses, Higgs masses, couplings and decay widths in the NMSSM", *Comput. Phys. Commun.* **175** (2006) 290, doi:10.1016/j.cpc.2006.04.004, arXiv:hep-ph/0508022.

[94] J. Baglio et al., "NMSSMCALC: A Program Package for the Calculation of Loop-Corrected Higgs Boson Masses and Decay Widths in the (Complex) NMSSM", *Comput. Phys. Commun.* **185** (2014), no. 12, 3372, doi:10.1016/j.cpc.2014.08.005, arXiv:1312.4788.

A The CMS Collaboration

Yerevan Physics Institute, Yerevan, Armenia
A. Tumasyan

Institut für Hochenergiephysik, Vienna, Austria
W. Adam, J.W. Andrejkovic, T. Bergauer, S. Chatterjee, K. Damanakis, M. Dragicevic, A. Escalante Del Valle, P.S. Hussain, M. Jeitler[1], N. Krammer, L. Lechner, D. Liko, I. Mikulec, P. Paulitsch, F.M. Pitters, J. Schieck[1], R. Schöfbeck, D. Schwarz, M. Sonawane, S. Templ, W. Waltenberger, C.-E. Wulz[1]

Universiteit Antwerpen, Antwerpen, Belgium
M.R. Darwish[2], T. Janssen, T. Kello[3], H. Rejeb Sfar, P. Van Mechelen

Vrije Universiteit Brussel, Brussel, Belgium
E.S. Bols, J. D'Hondt, A. De Moor, M. Delcourt, H. El Faham, S. Lowette, S. Moortgat, A. Morton, D. Müller, A.R. Sahasransu, S. Tavernier, W. Van Doninck, S. Van Putte, D. Vannerom

Université Libre de Bruxelles, Bruxelles, Belgium
B. Clerbaux, G. De Lentdecker, L. Favart, D. Hohov, J. Jaramillo, K. Lee, M. Mahdavikhorrami, I. Makarenko, A. Malara, S. Paredes, L. Pétré, N. Postiau, L. Thomas, M. Vanden Bemden, C. Vander Velde, P. Vanlaer

Ghent University, Ghent, Belgium
D. Dobur, J. Knolle, L. Lambrecht, G. Mestdach, C. Rendón, A. Samalan, K. Skovpen, M. Tytgat, N. Van Den Bossche, B. Vermassen, L. Wezenbeek

Université Catholique de Louvain, Louvain-la-Neuve, Belgium
A. Benecke, G. Bruno, F. Bury, C. Caputo, P. David, C. Delaere, I.S. Donertas, A. Giammanco, K. Jaffel, Sa. Jain, V. Lemaitre, K. Mondal, A. Taliercio, T.T. Tran, P. Vischia, S. Wertz

Centro Brasileiro de Pesquisas Fisicas, Rio de Janeiro, Brazil
G.A. Alves, E. Coelho, C. Hensel, A. Moraes, P. Rebello Teles

Universidade do Estado do Rio de Janeiro, Rio de Janeiro, Brazil
W.L. Aldá Júnior, M. Alves Gallo Pereira, M. Barroso Ferreira Filho, H. Brandao Malbouisson, W. Carvalho, J. Chinellato[4], E.M. Da Costa, G.G. Da Silveira[5], D. De Jesus Damiao, V. Dos Santos Sousa, S. Fonseca De Souza, J. Martins[6], C. Mora Herrera, K. Mota Amarilo, L. Mundim, H. Nogima, A. Santoro, S.M. Silva Do Amaral, A. Sznajder, M. Thiel, A. Vilela Pereira

Universidade Estadual Paulista, Universidade Federal do ABC, São Paulo, Brazil
C.A. Bernardes[5], L. Calligaris, T.R. Fernandez Perez Tomei, E.M. Gregores, P.G. Mercadante, S.F. Novaes, Sandra S. Padula

Institute for Nuclear Research and Nuclear Energy, Bulgarian Academy of Sciences, Sofia, Bulgaria
A. Aleksandrov, G. Antchev, R. Hadjiiska, P. Iaydjiev, M. Misheva, M. Rodozov, M. Shopova, G. Sultanov

University of Sofia, Sofia, Bulgaria
A. Dimitrov, T. Ivanov, L. Litov, B. Pavlov, P. Petkov, A. Petrov, E. Shumka

Instituto De Alta Investigación, Universidad de Tarapacá, Casilla 7 D, Arica, Chile

S. Thakur

Beihang University, Beijing, China
T. Cheng, T. Javaid[7], M. Mittal, L. Yuan

Department of Physics, Tsinghua University, Beijing, China
M. Ahmad, G. Bauer[8], Z. Hu, S. Lezki, K. Yi[8,9]

Institute of High Energy Physics, Beijing, China
G.M. Chen[7], H.S. Chen[7], M. Chen[7], F. Iemmi, C.H. Jiang, A. Kapoor, H. Liao, Z.-A. Liu[10], V. Milosevic, F. Monti, R. Sharma, J. Tao, J. Thomas-Wilsker, J. Wang, H. Zhang, J. Zhao

State Key Laboratory of Nuclear Physics and Technology, Peking University, Beijing, China
A. Agapitos, Y. An, Y. Ban, A. Levin, C. Li, Q. Li, X. Lyu, Y. Mao, S.J. Qian, X. Sun, D. Wang, J. Xiao, H. Yang

Sun Yat-Sen University, Guangzhou, China
M. Lu, Z. You

University of Science and Technology of China, Hefei, China
N. Lu

Institute of Modern Physics and Key Laboratory of Nuclear Physics and Ion-beam Application (MOE) - Fudan University, Shanghai, China
X. Gao[3], D. Leggat, H. Okawa, Y. Zhang

Zhejiang University, Hangzhou, Zhejiang, China
Z. Lin, C. Lu, M. Xiao

Universidad de Los Andes, Bogota, Colombia
C. Avila, D.A. Barbosa Trujillo, A. Cabrera, C. Florez, J. Fraga

Universidad de Antioquia, Medellin, Colombia
J. Mejia Guisao, F. Ramirez, M. Rodriguez, J.D. Ruiz Alvarez

University of Split, Faculty of Electrical Engineering, Mechanical Engineering and Naval Architecture, Split, Croatia
D. Giljanovic, N. Godinovic, D. Lelas, I. Puljak

University of Split, Faculty of Science, Split, Croatia
Z. Antunovic, M. Kovac, T. Sculac

Institute Rudjer Boskovic, Zagreb, Croatia
V. Brigljevic, B.K. Chitroda, D. Ferencek, D. Majumder, S. Mishra, M. Roguljic, A. Starodumov[11], T. Susa

University of Cyprus, Nicosia, Cyprus
A. Attikis, K. Christoforou, M. Kolosova, S. Konstantinou, J. Mousa, C. Nicolaou, F. Ptochos, P.A. Razis, H. Rykaczewski, H. Saka, A. Stepennov

Charles University, Prague, Czech Republic
M. Finger, M. Finger Jr., A. Kveton

Escuela Politecnica Nacional, Quito, Ecuador
E. Ayala

Universidad San Francisco de Quito, Quito, Ecuador

E. Carrera Jarrin

Academy of Scientific Research and Technology of the Arab Republic of Egypt, Egyptian Network of High Energy Physics, Cairo, Egypt
S. Elgammal[12], A. Ellithi Kamel[13]

Center for High Energy Physics (CHEP-FU), Fayoum University, El-Fayoum, Egypt
A. Lotfy, M.A. Mahmoud

National Institute of Chemical Physics and Biophysics, Tallinn, Estonia
S. Bhowmik, R.K. Dewanjee, K. Ehataht, M. Kadastik, T. Lange, S. Nandan, C. Nielsen, J. Pata, M. Raidal, L. Tani, C. Veelken

Department of Physics, University of Helsinki, Helsinki, Finland
P. Eerola, H. Kirschenmann, K. Osterberg, M. Voutilainen

Helsinki Institute of Physics, Helsinki, Finland
S. Bharthuar, E. Brücken, F. Garcia, J. Havukainen, M.S. Kim, R. Kinnunen, T. Lampén, K. Lassila-Perini, S. Lehti, T. Lindén, M. Lotti, L. Martikainen, M. Myllymäki, J. Ott, M.m. Rantanen, H. Siikonen, E. Tuominen, J. Tuominiemi

Lappeenranta-Lahti University of Technology, Lappeenranta, Finland
P. Luukka, H. Petrow, T. Tuuva

IRFU, CEA, Université Paris-Saclay, Gif-sur-Yvette, France
C. Amendola, M. Besancon, F. Couderc, M. Dejardin, D. Denegri, J.L. Faure, F. Ferri, S. Ganjour, P. Gras, G. Hamel de Monchenault, V. Lohezic, J. Malcles, J. Rander, A. Rosowsky, M.Ö. Sahin, A. Savoy-Navarro[14], P. Simkina, M. Titov

Laboratoire Leprince-Ringuet, CNRS/IN2P3, Ecole Polytechnique, Institut Polytechnique de Paris, Palaiseau, France
C. Baldenegro Barrera, F. Beaudette, A. Buchot Perraguin, P. Busson, A. Cappati, C. Charlot, F. Damas, O. Davignon, B. Diab, G. Falmagne, B.A. Fontana Santos Alves, S. Ghosh, R. Granier de Cassagnac, A. Hakimi, B. Harikrishnan, G. Liu, J. Motta, M. Nguyen, C. Ochando, L. Portales, R. Salerno, U. Sarkar, J.B. Sauvan, Y. Sirois, A. Tarabini, E. Vernazza, A. Zabi, A. Zghiche

Université de Strasbourg, CNRS, IPHC UMR 7178, Strasbourg, France
J.-L. Agram[15], J. Andrea, D. Apparu, D. Bloch, G. Bourgatte, J.-M. Brom, E.C. Chabert, C. Collard, D. Darej, U. Goerlach, C. Grimault, A.-C. Le Bihan, P. Van Hove

Institut de Physique des 2 Infinis de Lyon (IP2I), Villeurbanne, France
S. Beauceron, B. Blancon, G. Boudoul, A. Carle, N. Chanon, J. Choi, D. Contardo, P. Depasse, C. Dozen[16], H. El Mamouni, J. Fay, S. Gascon, M. Gouzevitch, G. Grenier, B. Ille, I.B. Laktineh, M. Lethuillier, L. Mirabito, S. Perries, L. Torterotot, M. Vander Donckt, P. Verdier, S. Viret

Georgian Technical University, Tbilisi, Georgia
D. Chokheli, I. Lomidze, Z. Tsamalaidze[11]

RWTH Aachen University, I. Physikalisches Institut, Aachen, Germany
V. Botta, L. Feld, K. Klein, M. Lipinski, D. Meuser, A. Pauls, N. Röwert, M. Teroerde

RWTH Aachen University, III. Physikalisches Institut A, Aachen, Germany

S. Diekmann, A. Dodonova, N. Eich, D. Eliseev, M. Erdmann, P. Fackeldey, D. Fasanella, B. Fischer, T. Hebbeker, K. Hoepfner, F. Ivone, M.y. Lee, L. Mastrolorenzo, M. Merschmeyer, A. Meyer, S. Mondal, S. Mukherjee, D. Noll, A. Novak, F. Nowotny, A. Pozdnyakov, Y. Rath, W. Redjeb, H. Reithler, A. Schmidt, S.C. Schuler, A. Sharma, A. Stein, F. Torres Da Silva De Araujo[17], L. Vigilante, S. Wiedenbeck, S. Zaleski

RWTH Aachen University, III. Physikalisches Institut B, Aachen, Germany
C. Dziwok, G. Flügge, W. Haj Ahmad[18], O. Hlushchenko, T. Kress, A. Nowack, O. Pooth, A. Stahl, T. Ziemons, A. Zotz

Deutsches Elektronen-Synchrotron, Hamburg, Germany
H. Aarup Petersen, M. Aldaya Martin, P. Asmuss, S. Baxter, M. Bayatmakou, H. Becerril Gonzalez, O. Behnke, A. Bermúdez Martínez, S. Bhattacharya, A.A. Bin Anuar, F. Blekman[19], K. Borras[20], D. Brunner, A. Campbell, A. Cardini, C. Cheng, F. Colombina, S. Consuegra Rodríguez, G. Correia Silva, M. De Silva, L. Didukh, G. Eckerlin, D. Eckstein, L.I. Estevez Banos, O. Filatov, E. Gallo[19], A. Geiser, A. Giraldi, G. Greau, A. Grohsjean, V. Guglielmi, M. Guthoff, A. Jafari[21], N.Z. Jomhari, B. Kaech, M. Kasemann, H. Kaveh, C. Kleinwort, R. Kogler, M. Komm, D. Krücker, W. Lange, D. Leyva Pernia, K. Lipka[22], W. Lohmann[23], R. Mankel, I.-A. Melzer-Pellmann, M. Mendizabal Morentin, J. Metwally, A.B. Meyer, G. Milella, M. Mormile, A. Mussgiller, A. Nürnberg, Y. Otarid, D. Pérez Adán, E. Ranken, A. Raspereza, B. Ribeiro Lopes, J. Rübenach, A. Saggio, A. Saibel, M. Savitskyi, M. Scham[24,20], V. Scheurer, S. Schnake[20], P. Schütze, C. Schwanenberger[19], M. Shchedrolosiev, R.E. Sosa Ricardo, D. Stafford, N. Tonon[†], M. Van De Klundert, F. Vazzoler, A. Ventura Barroso, R. Walsh, D. Walter, Q. Wang, Y. Wen, K. Wichmann, L. Wiens[20], C. Wissing, S. Wuchterl, Y. Yang, A. Zimermmane Castro Santos

University of Hamburg, Hamburg, Germany
A. Albrecht, S. Albrecht, M. Antonello, S. Bein, L. Benato, M. Bonanomi, P. Connor, K. De Leo, M. Eich, K. El Morabit, F. Feindt, A. Fröhlich, C. Garbers, E. Garutti, M. Hajheidari, J. Haller, A. Hinzmann, H.R. Jabusch, G. Kasieczka, P. Keicher, R. Klanner, W. Korcari, T. Kramer, V. Kutzner, F. Labe, J. Lange, A. Lobanov, C. Matthies, A. Mehta, L. Moureaux, M. Mrowietz, A. Nigamova, Y. Nissan, A. Paasch, K.J. Pena Rodriguez, T. Quadfasel, M. Rieger, O. Rieger, D. Savoiu, J. Schindler, P. Schleper, M. Schröder, J. Schwandt, M. Sommerhalder, H. Stadie, G. Steinbrück, A. Tews, M. Wolf

Karlsruher Institut fuer Technologie, Karlsruhe, Germany
S. Brommer, M. Burkart, E. Butz, T. Chwalek, A. Dierlamm, A. Droll, N. Faltermann, M. Giffels, J.O. Gosewisch, A. Gottmann, F. Hartmann[25], M. Horzela, U. Husemann, M. Klute, R. Koppenhöfer, M. Link, A. Lintuluoto, S. Maier, S. Mitra, Th. Müller, M. Neukum, M. Oh, G. Quast, K. Rabbertz, J. Rauser, I. Shvetsov, H.J. Simonis, N. Trevisani, R. Ulrich, J. van der Linden, R.F. Von Cube, M. Wassmer, S. Wieland, R. Wolf, S. Wozniewski, S. Wunsch, X. Zuo

Institute of Nuclear and Particle Physics (INPP), NCSR Demokritos, Aghia Paraskevi, Greece
G. Anagnostou, P. Assiouras, G. Daskalakis, A. Kyriakis, A. Stakia

National and Kapodistrian University of Athens, Athens, Greece
M. Diamantopoulou, D. Karasavvas, P. Kontaxakis, A. Manousakis-Katsikakis, A. Panagiotou, I. Papavergou, N. Saoulidou, K. Theofilatos, E. Tziaferi, K. Vellidis, I. Zisopoulos

National Technical University of Athens, Athens, Greece
G. Bakas, T. Chatzistavrou, K. Kousouris, I. Papakrivopoulos, G. Tsipolitis, A. Zacharopoulou

University of Ioánnina, Ioánnina, Greece
K. Adamidis, I. Bestintzanos, I. Evangelou, C. Foudas, P. Gianneios, C. Kamtsikis, P. Katsoulis, P. Kokkas, P.G. Kosmoglou Kioseoglou, N. Manthos, I. Papadopoulos, J. Strologas

MTA-ELTE Lendület CMS Particle and Nuclear Physics Group, Eötvös Loránd University, Budapest, Hungary
M. Csanád, K. Farkas, M.M.A. Gadallah[26], S. Lökös[27], P. Major, K. Mandal, G. Pásztor, A.J. Rádl[28], O. Surányi, G.I. Veres

Wigner Research Centre for Physics, Budapest, Hungary
M. Bartók[29], G. Bencze, C. Hajdu, D. Horvath[30,31], F. Sikler, V. Veszpremi

Institute of Nuclear Research ATOMKI, Debrecen, Hungary
N. Beni, S. Czellar, J. Karancsi[29], J. Molnar, Z. Szillasi, D. Teyssier

Institute of Physics, University of Debrecen, Debrecen, Hungary
P. Raics, B. Ujvari[32], G. Zilizi

Karoly Robert Campus, MATE Institute of Technology, Gyongyos, Hungary
T. Csorgo[28], F. Nemes[28], T. Novak

Panjab University, Chandigarh, India
J. Babbar, S. Bansal, S.B. Beri, V. Bhatnagar, G. Chaudhary, S. Chauhan, N. Dhingra[33], R. Gupta, A. Kaur, A. Kaur, H. Kaur, M. Kaur, S. Kumar, P. Kumari, M. Meena, K. Sandeep, T. Sheokand, J.B. Singh[34], A. Singla, A. K. Virdi

University of Delhi, Delhi, India
A. Ahmed, A. Bhardwaj, A. Chhetri, B.C. Choudhary, A. Kumar, M. Naimuddin, K. Ranjan, S. Saumya

Saha Institute of Nuclear Physics, HBNI, Kolkata, India
S. Baradia, S. Barman[35], S. Bhattacharya, D. Bhowmik, S. Dutta, S. Dutta, B. Gomber[36], M. Maity[35], P. Palit, G. Saha, B. Sahu, S. Sarkar

Indian Institute of Technology Madras, Madras, India
P.K. Behera, S.C. Behera, S. Chatterjee, P. Kalbhor, J.R. Komaragiri[37], D. Kumar[37], A. Muhammad, L. Panwar[37], R. Pradhan, P.R. Pujahari, N.R. Saha, A. Sharma, A.K. Sikdar, S. Verma

Bhabha Atomic Research Centre, Mumbai, India
K. Naskar[38]

Tata Institute of Fundamental Research-A, Mumbai, India
T. Aziz, I. Das, S. Dugad, M. Kumar, G.B. Mohanty, P. Suryadevara

Tata Institute of Fundamental Research-B, Mumbai, India
S. Banerjee, M. Guchait, S. Karmakar, S. Kumar, G. Majumder, K. Mazumdar, S. Mukherjee, A. Thachayath

National Institute of Science Education and Research, An OCC of Homi Bhabha National Institute, Bhubaneswar, Odisha, India
S. Bahinipati[39], A.K. Das, C. Kar, P. Mal, T. Mishra, V.K. Muraleedharan Nair Bindhu[40], A. Nayak[40], P. Saha, S.K. Swain, D. Vats[40]

Indian Institute of Science Education and Research (IISER), Pune, India
A. Alpana, S. Dube, B. Kansal, A. Laha, S. Pandey, A. Rastogi, S. Sharma

Isfahan University of Technology, Isfahan, Iran
H. Bakhshiansohi[41,42], E. Khazaie[42], M. Zeinali[43]

Institute for Research in Fundamental Sciences (IPM), Tehran, Iran
S. Chenarani[44], S.M. Etesami, M. Khakzad, M. Mohammadi Najafabadi

University College Dublin, Dublin, Ireland
M. Grunewald

INFN Sezione di Bari[a], Università di Bari[b], Politecnico di Bari[c], Bari, Italy
M. Abbrescia[a,b], R. Aly[a,b,45], C. Aruta[a,b], A. Colaleo[a], D. Creanza[a,c], L. Cristella[a,b], N. De Filippis[a,c], M. De Palma[a,b], A. Di Florio[a,b], W. Elmetenawee[a,b], F. Errico[a,b], L. Fiore[a], G. Iaselli[a,c], G. Maggi[a,c], M. Maggi[a], I. Margjeka[a,b], V. Mastrapasqua[a,b], S. My[a,b], S. Nuzzo[a,b], A. Pellecchia[a,b], A. Pompili[a,b], G. Pugliese[a,c], R. Radogna[a], D. Ramos[a], A. Ranieri[a], G. Selvaggi[a,b], L. Silvestris[a], F.M. Simone[a,b], Ü. Sözbilir[a], A. Stamerra[a], R. Venditti[a], P. Verwilligen[a]

INFN Sezione di Bologna[a], Università di Bologna[b], Bologna, Italy
G. Abbiendi[a], C. Battilana[a,b], D. Bonacorsi[a,b], L. Borgonovi[a], L. Brigliadori[a], R. Campanini[a,b], P. Capiluppi[a,b], A. Castro[a,b], F.R. Cavallo[a], M. Cuffiani[a,b], G.M. Dallavalle[a], T. Diotalevi[a,b], F. Fabbri[a], A. Fanfani[a,b], P. Giacomelli[a], L. Giommi[a,b], C. Grandi[a], L. Guiducci[a,b], S. Lo Meo[a,46], L. Lunerti[a,b], S. Marcellini[a], G. Masetti[a], F.L. Navarria[a,b], A. Perrotta[a], F. Primavera[a,b], A.M. Rossi[a,b], T. Rovelli[a,b], G.P. Siroli[a,b]

INFN Sezione di Catania[a], Università di Catania[b], Catania, Italy
S. Costa[a,b,47], A. Di Mattia[a], R. Potenza[a,b], A. Tricomi[a,b,47], C. Tuve[a,b]

INFN Sezione di Firenze[a], Università di Firenze[b], Firenze, Italy
G. Barbagli[a], G. Bardelli[a,b], B. Camaiani[a,b], A. Cassese[a], R. Ceccarelli[a,b], V. Ciulli[a,b], C. Civinini[a], R. D'Alessandro[a,b], E. Focardi[a,b], G. Latino[a,b], P. Lenzi[a,b], M. Lizzo[a,b], M. Meschini[a], S. Paoletti[a], R. Seidita[a,b], G. Sguazzoni[a], L. Viliani[a]

INFN Laboratori Nazionali di Frascati, Frascati, Italy
L. Benussi, S. Bianco, S. Meola[48], D. Piccolo

INFN Sezione di Genova[a], Università di Genova[b], Genova, Italy
M. Bozzo[a,b], P. Chatagnon[a], F. Ferro[a], E. Robutti[a], S. Tosi[a,b]

INFN Sezione di Milano-Bicocca[a], Università di Milano-Bicocca[b], Milano, Italy
A. Benaglia[a], G. Boldrini[a], F. Brivio[a,b], F. Cetorelli[a,b], F. De Guio[a,b],

M.E. Dinardo[a,b], P. Dini[a], S. Gennai[a], A. Ghezzi[a,b], P. Govoni[a,b], L. Guzzi[a,b], M.T. Lucchini[a,b], M. Malberti[a], S. Malvezzi[a], A. Massironi[a], D. Menasce[a], L. Moroni[a], M. Paganoni[a,b], D. Pedrini[a], B.S. Pinolini[a], S. Ragazzi[a,b], N. Redaelli[a], T. Tabarelli de Fatis[a,b], D. Zuolo[a,b]

INFN Sezione di Napoli[a], Università di Napoli 'Federico II'[b], Napoli, Italy; Università della Basilicata[c], Potenza, Italy; Università G. Marconi[d], Roma, Italy
S. Buontempo[a], F. Carnevali[a,b], N. Cavallo[a,c], A. De Iorio[a,b], F. Fabozzi[a,c], A.O.M. Iorio[a,b], L. Lista[a,b,49], P. Paolucci[a,25], B. Rossi[a], C. Sciacca[a,b]

INFN Sezione di Padova[a], Università di Padova[b], Padova, Italy; Università di Trento[c], Trento, Italy
P. Azzi[a], N. Bacchetta[a,50], D. Bisello[a,b], P. Bortignon[a], A. Bragagnolo[a,b], R. Carlin[a,b], P. Checchia[a], T. Dorigo[a], F. Gasparini[a,b], U. Gasparini[a,b], G. Grosso[a], L. Layer[a,51], E. Lusiani[a], M. Margoni[a,b], A.T. Meneguzzo[a,b], J. Pazzini[a,b], P. Ronchese[a,b], R. Rossin[a,b], G. Strong[a], M. Tosi[a,b], S. Ventura[a], H. Yarar[a,b], M. Zanetti[a,b], P. Zotto[a,b], A. Zucchetta[a,b], G. Zumerle[a,b]

INFN Sezione di Pavia[a], Università di Pavia[b], Pavia, Italy
S. Abu Zeid[a,52], C. Aimè[a,b], A. Braghieri[a], S. Calzaferri[a,b], D. Fiorina[a,b], P. Montagna[a,b], V. Re[a], C. Riccardi[a,b], P. Salvini[a], I. Vai[a], P. Vitulo[a,b]

INFN Sezione di Perugia[a], Università di Perugia[b], Perugia, Italy
P. Asenov[a,53], G.M. Bilei[a], D. Ciangottini[a,b], L. Fanò[a,b], M. Magherini[a,b], G. Mantovani[a,b], V. Mariani[a,b], M. Menichelli[a], F. Moscatelli[a,53], A. Piccinelli[a,b], M. Presilla[a,b], A. Rossi[a,b], A. Santocchia[a,b], D. Spiga[a], T. Tedeschi[a,b]

INFN Sezione di Pisa[a], Università di Pisa[b], Scuola Normale Superiore di Pisa[c], Pisa, Italy; Università di Siena[d], Siena, Italy
P. Azzurri[a], G. Bagliesi[a], V. Bertacchi[a,c], R. Bhattacharya[a], L. Bianchini[a,b], T. Boccali[a], E. Bossini[a,b], D. Bruschini[a,c], R. Castaldi[a], M.A. Ciocci[a,b], V. D'Amante[a,d], R. Dell'Orso[a], S. Donato[a], A. Giassi[a], F. Ligabue[a,c], D. Matos Figueiredo[a], A. Messineo[a,b], M. Musich[a,b], F. Palla[a], S. Parolia[a], G. Ramirez-Sanchez[a,c], A. Rizzi[a,b], G. Rolandi[a,c], S. Roy Chowdhury[a], T. Sarkar[a], A. Scribano[a], P. Spagnolo[a], R. Tenchini[a], G. Tonelli[a,b], N. Turini[a,d], A. Venturi[a], P.G. Verdini[a]

INFN Sezione di Roma[a], Sapienza Università di Roma[b], Roma, Italy
P. Barria[a], M. Campana[a,b], F. Cavallari[a], D. Del Re[a,b], E. Di Marco[a], M. Diemoz[a], E. Longo[a,b], P. Meridiani[a], G. Organtini[a,b], F. Pandolfi[a], R. Paramatti[a,b], C. Quaranta[a,b], S. Rahatlou[a,b], C. Rovelli[a], F. Santanastasio[a,b], L. Soffi[a], R. Tramontano[a,b]

INFN Sezione di Torino[a], Università di Torino[b], Torino, Italy; Università del Piemonte Orientale[c], Novara, Italy
N. Amapane[a,b], R. Arcidiacono[a,c], S. Argiro[a,b], M. Arneodo[a,c], N. Bartosik[a], R. Bellan[a,b], A. Bellora[a,b], C. Biino[a], N. Cartiglia[a], M. Costa[a,b], R. Covarelli[a,b], N. Demaria[a], M. Grippo[a,b], B. Kiani[a,b], F. Legger[a], C. Mariotti[a], S. Maselli[a], A. Mecca[a,b], E. Migliore[a,b], E. Monteil[a,b], M. Monteno[a], R. Mulargia[a], M.M. Obertino[a,b], G. Ortona[a], L. Pacher[a,b], N. Pastrone[a], M. Pelliccioni[a], M. Ruspa[a,c], K. Shchelina[a], F. Siviero[a,b], V. Sola[a,b], A. Solano[a,b], D. Soldi[a,b], A. Staiano[a], M. Tornago[a,b], D. Trocino[a], G. Umoret[a,b], A. Vagnerini[a,b], E. Vlasov[a]

INFN Sezione di Trieste[a], Università di Trieste[b], Trieste, Italy
S. Belforte[a], V. Candelise[a,b], M. Casarsa[a], F. Cossutti[a], G. Della Ricca[a,b], G. Sorrentino[a,b]

Kyungpook National University, Daegu, Korea
S. Dogra, C. Huh, B. Kim, D.H. Kim, G.N. Kim, J. Kim, J. Lee, S.W. Lee, C.S. Moon, Y.D. Oh, S.I. Pak, M.S. Ryu, S. Sekmen, Y.C. Yang

Chonnam National University, Institute for Universe and Elementary Particles, Kwangju, Korea
H. Kim, D.H. Moon

Hanyang University, Seoul, Korea
E. Asilar, T.J. Kim, J. Park

Korea University, Seoul, Korea
S. Choi, S. Han, B. Hong, K. Lee, K.S. Lee, J. Lim, J. Park, S.K. Park, J. Yoo

Kyung Hee University, Department of Physics, Seoul, Korea
J. Goh

Sejong University, Seoul, Korea
H. S. Kim, Y. Kim, S. Lee

Seoul National University, Seoul, Korea
J. Almond, J.H. Bhyun, J. Choi, S. Jeon, J. Kim, J.S. Kim, S. Ko, H. Kwon, H. Lee, S. Lee, B.H. Oh, S.B. Oh, H. Seo, U.K. Yang, I. Yoon

University of Seoul, Seoul, Korea
W. Jang, D.Y. Kang, Y. Kang, D. Kim, S. Kim, B. Ko, J.S.H. Lee, Y. Lee, J.A. Merlin, I.C. Park, Y. Roh, D. Song, I.J. Watson, S. Yang

Yonsei University, Department of Physics, Seoul, Korea
S. Ha, H.D. Yoo

Sungkyunkwan University, Suwon, Korea
M. Choi, M.R. Kim, H. Lee, Y. Lee, Y. Lee, I. Yu

College of Engineering and Technology, American University of the Middle East (AUM), Dasman, Kuwait
T. Beyrouthy, Y. Maghrbi

Riga Technical University, Riga, Latvia
K. Dreimanis, G. Pikurs, A. Potrebko, M. Seidel, V. Veckalns[54]

Vilnius University, Vilnius, Lithuania
M. Ambrozas, A. Carvalho Antunes De Oliveira, A. Juodagalvis, A. Rinkevicius, G. Tamulaitis

National Centre for Particle Physics, Universiti Malaya, Kuala Lumpur, Malaysia
N. Bin Norjoharuddeen, S.Y. Hoh[55], I. Yusuff[55], Z. Zolkapli

Universidad de Sonora (UNISON), Hermosillo, Mexico
J.F. Benitez, A. Castaneda Hernandez, H.A. Encinas Acosta, L.G. Gallegos Maríñez, M. León Coello, J.A. Murillo Quijada, A. Sehrawat, L. Valencia Palomo

Centro de Investigacion y de Estudios Avanzados del IPN, Mexico City, Mexico

G. Ayala, H. Castilla-Valdez, I. Heredia-De La Cruz[56], R. Lopez-Fernandez, C.A. Mondragon Herrera, D.A. Perez Navarro, A. Sánchez Hernández

Universidad Iberoamericana, Mexico City, Mexico
C. Oropeza Barrera, F. Vazquez Valencia

Benemerita Universidad Autonoma de Puebla, Puebla, Mexico
I. Pedraza, H.A. Salazar Ibarguen, C. Uribe Estrada

University of Montenegro, Podgorica, Montenegro
I. Bubanja, J. Mijuskovic[57], N. Raicevic

National Centre for Physics, Quaid-I-Azam University, Islamabad, Pakistan
A. Ahmad, M.I. Asghar, A. Awais, M.I.M. Awan, M. Gul, H.R. Hoorani, W.A. Khan

AGH University of Krakow, Faculty of Computer Science, Electronics and Telecommunications, Krakow, Poland
V. Avati, L. Grzanka, M. Malawski

National Centre for Nuclear Research, Swierk, Poland
H. Bialkowska, M. Bluj, B. Boimska, M. Górski, M. Kazana, M. Szleper, P. Zalewski

Institute of Experimental Physics, Faculty of Physics, University of Warsaw, Warsaw, Poland
K. Bunkowski, K. Doroba, A. Kalinowski, M. Konecki, J. Krolikowski

Laboratório de Instrumentação e Física Experimental de Partículas, Lisboa, Portugal
M. Araujo, P. Bargassa, D. Bastos, A. Boletti, P. Faccioli, M. Gallinaro, J. Hollar, N. Leonardo, T. Niknejad, M. Pisano, J. Seixas, J. Varela

VINCA Institute of Nuclear Sciences, University of Belgrade, Belgrade, Serbia
P. Adzic[58], M. Dordevic, P. Milenovic, J. Milosevic

Centro de Investigaciones Energéticas Medioambientales y Tecnológicas (CIEMAT), Madrid, Spain
M. Aguilar-Benitez, J. Alcaraz Maestre, M. Barrio Luna, Cristina F. Bedoya, M. Cepeda, M. Cerrada, N. Colino, B. De La Cruz, A. Delgado Peris, D. Fernández Del Val, J.P. Fernández Ramos, J. Flix, M.C. Fouz, O. Gonzalez Lopez, S. Goy Lopez, J.M. Hernandez, M.I. Josa, J. León Holgado, D. Moran, C. Perez Dengra, A. Pérez-Calero Yzquierdo, J. Puerta Pelayo, I. Redondo, D.D. Redondo Ferrero, L. Romero, S. Sánchez Navas, J. Sastre, L. Urda Gómez, J. Vazquez Escobar, C. Willmott

Universidad Autónoma de Madrid, Madrid, Spain
J.F. de Trocóniz

Universidad de Oviedo, Instituto Universitario de Ciencias y Tecnologías Espaciales de Asturias (ICTEA), Oviedo, Spain
B. Alvarez Gonzalez, J. Cuevas, J. Fernandez Menendez, S. Folgueras, I. Gonzalez Caballero, J.R. González Fernández, E. Palencia Cortezon, C. Ramón Álvarez, V. Rodríguez Bouza, A. Soto Rodríguez, A. Trapote, C. Vico Villalba

Instituto de Física de Cantabria (IFCA), CSIC-Universidad de Cantabria, Santander, Spain
J.A. Brochero Cifuentes, I.J. Cabrillo, A. Calderon, J. Duarte Campderros, M. Fernandez, C. Fernandez Madrazo, A. García Alonso, G. Gomez, C. Lasaosa García, C. Martinez Rivero, P. Martinez Ruiz del Arbol, F. Matorras, P. Matorras Cuevas, J. Piedra Gomez, C. Prieels, L. Scodellaro, I. Vila, J.M. Vizan Garcia

University of Colombo, Colombo, Sri Lanka
M.K. Jayananda, B. Kailasapathy[59], D.U.J. Sonnadara, D.D.C. Wickramarathna

University of Ruhuna, Department of Physics, Matara, Sri Lanka
W.G.D. Dharmaratna, K. Liyanage, N. Perera, N. Wickramage

CERN, European Organization for Nuclear Research, Geneva, Switzerland
D. Abbaneo, J. Alimena, E. Auffray, G. Auzinger, J. Baechler, P. Baillon[†], D. Barney, J. Bendavid, M. Bianco, B. Bilin, A. Bocci, E. Brondolin, C. Caillol, T. Camporesi, G. Cerminara, N. Chernyavskaya, S.S. Chhibra, S. Choudhury, M. Cipriani, D. d'Enterria, A. Dabrowski, A. David, A. De Roeck, M.M. Defranchis, M. Deile, M. Dobson, M. Dünser, N. Dupont, F. Fallavollita[60], A. Florent, L. Forthomme, G. Franzoni, W. Funk, S. Ghosh, S. Giani, D. Gigi, K. Gill, F. Glege, L. Gouskos, E. Govorkova, M. Haranko, J. Hegeman, V. Innocente, T. James, P. Janot, J. Kaspar, J. Kieseler, N. Kratochwil, S. Laurila, P. Lecoq, E. Leutgeb, C. Lourenço, B. Maier, L. Malgeri, M. Mannelli, A.C. Marini, F. Meijers, S. Mersi, E. Meschi, F. Moortgat, M. Mulders, S. Orfanelli, L. Orsini, F. Pantaleo, E. Perez, M. Peruzzi, A. Petrilli, G. Petrucciani, A. Pfeiffer, M. Pierini, D. Piparo, M. Pitt, H. Qu, T. Quast, D. Rabady, A. Racz, G. Reales Gutiérrez, M. Rovere, H. Sakulin, J. Salfeld-Nebgen, S. Scarfi, M. Selvaggi, A. Sharma, P. Silva, P. Sphicas[61], A.G. Stahl Leiton, S. Summers, K. Tatar, D. Treille, P. Tropea, A. Tsirou, J. Wanczyk[62], K.A. Wozniak, W.D. Zeuner

Paul Scherrer Institut, Villigen, Switzerland
L. Caminada[63], A. Ebrahimi, W. Erdmann, R. Horisberger, Q. Ingram, H.C. Kaestli, D. Kotlinski, C. Lange, M. Missiroli[63], L. Noehte[63], T. Rohe

ETH Zurich - Institute for Particle Physics and Astrophysics (IPA), Zurich, Switzerland
T.K. Aarrestad, K. Androsov[62], M. Backhaus, P. Berger, A. Calandri, K. Datta, A. De Cosa, G. Dissertori, M. Dittmar, M. Donegà, F. Eble, M. Galli, K. Gedia, F. Glessgen, T.A. Gómez Espinosa, C. Grab, D. Hits, W. Lustermann, A.-M. Lyon, R.A. Manzoni, L. Marchese, C. Martin Perez, A. Mascellani[62], F. Nessi-Tedaldi, J. Niedziela, F. Pauss, V. Perovic, S. Pigazzini, M.G. Ratti, M. Reichmann, C. Reissel, T. Reitenspiess, B. Ristic, F. Riti, D. Ruini, D.A. Sanz Becerra, J. Steggemann[62], D. Valsecchi[25], R. Wallny

Universität Zürich, Zurich, Switzerland
C. Amsler[64], P. Bärtschi, C. Botta, D. Brzhechko, M.F. Canelli, K. Cormier, A. De Wit, R. Del Burgo, J.K. Heikkilä, M. Huwiler, W. Jin, A. Jofrehei, B. Kilminster, S. Leontsinis, S.P. Liechti, A. Macchiolo, P. Meiring, V.M. Mikuni, U. Molinatti, I. Neutelings, A. Reimers, P. Robmann, S. Sanchez Cruz, K. Schweiger, M. Senger, Y. Takahashi

National Central University, Chung-Li, Taiwan
C. Adloff[65], C.M. Kuo, W. Lin, P.K. Rout, P.C. Tiwari[37], S.S. Yu

National Taiwan University (NTU), Taipei, Taiwan
L. Ceard, Y. Chao, K.F. Chen, P.s. Chen, H. Cheng, W.-S. Hou, R. Khurana, G. Kole, Y.y. Li, R.-S. Lu, E. Paganis, A. Psallidas, A. Steen, H.y. Wu, E. Yazgan

High Energy Physics Research Unit, Department of Physics, Faculty of Science, Chulalongkorn University, Bangkok, Thailand
C. Asawatangtrakuldee, N. Srimanobhas, V. Wachirapusitanand

Çukurova University, Physics Department, Science and Art Faculty, Adana, Turkey
D. Agyel, F. Boran, Z.S. Demiroglu, F. Dolek, I. Dumanoglu[66], E. Eskut, Y. Guler[67], E. Gurpinar Guler[67], C. Isik, O. Kara, A. Kayis Topaksu, U. Kiminsu, G. Onengut, K. Ozdemir[68], A. Polatoz, A.E. Simsek, B. Tali[69], U.G. Tok, S. Turkcapar, E. Uslan, I.S. Zorbakir

Middle East Technical University, Physics Department, Ankara, Turkey
G. Karapinar[70], K. Ocalan[71], M. Yalvac[72]

Bogazici University, Istanbul, Turkey
B. Akgun, I.O. Atakisi, E. Gülmez, M. Kaya[73], O. Kaya[74], S. Tekten[75]

Istanbul Technical University, Istanbul, Turkey
A. Cakir, K. Cankocak[66], Y. Komurcu, S. Sen[66]

Istanbul University, Istanbul, Turkey
O. Aydilek, S. Cerci[69], B. Hacisahinoglu, I. Hos[76], B. Isildak[77], B. Kaynak, S. Ozkorucuklu, C. Simsek, D. Sunar Cerci[69]

Institute for Scintillation Materials of National Academy of Science of Ukraine, Kharkiv, Ukraine
B. Grynyov

National Science Centre, Kharkiv Institute of Physics and Technology, Kharkiv, Ukraine
L. Levchuk

University of Bristol, Bristol, United Kingdom
D. Anthony, J.J. Brooke, A. Bundock, E. Clement, D. Cussans, H. Flacher, M. Glowacki, J. Goldstein, H.F. Heath, L. Kreczko, B. Krikler, S. Paramesvaran, S. Seif El Nasr-Storey, V.J. Smith, N. Stylianou[78], K. Walkingshaw Pass, R. White

Rutherford Appleton Laboratory, Didcot, United Kingdom
A.H. Ball, K.W. Bell, A. Belyaev[79], C. Brew, R.M. Brown, D.J.A. Cockerill, C. Cooke, K.V. Ellis, K. Harder, S. Harper, M.-L. Holmberg[80], Sh. Jain, J. Linacre, K. Manolopoulos, D.M. Newbold, E. Olaiya, D. Petyt, T. Reis, G. Salvi, T. Schuh, C.H. Shepherd-Themistocleous, I.R. Tomalin, T. Williams

Imperial College, London, United Kingdom
R. Bainbridge, P. Bloch, S. Bonomally, J. Borg, C.E. Brown, O. Buchmuller, V. Cacchio, C.A. Carrillo Montoya, V. Cepaitis, G.S. Chahal[81], D. Colling, J.S. Dancu, P. Dauncey, G. Davies, J. Davies, M. Della Negra, S. Fayer, G. Fedi, G. Hall, M.H. Hassanshahi, A. Howard, G. Iles, J. Langford, L. Lyons, A.-M. Magnan, S. Malik, A. Martelli, M. Mieskolainen, D.G. Monk, J. Nash[82], M. Pesaresi, B.C. Radburn-Smith, D.M. Raymond, A. Richards, A. Rose, E. Scott, C. Seez, R. Shukla, A. Tapper, K. Uchida, G.P. Uttley, L.H. Vage, T. Virdee[25], M. Vojinovic, N. Wardle, S.N. Webb, D. Winterbottom

Brunel University, Uxbridge, United Kingdom
K. Coldham, J.E. Cole, A. Khan, P. Kyberd, I.D. Reid

Baylor University, Waco, Texas, USA
S. Abdullin, A. Brinkerhoff, B. Caraway, J. Dittmann, K. Hatakeyama, A.R. Kanuganti, B. McMaster, M. Saunders, S. Sawant, C. Sutantawibul, M. Toms, J. Wilson

Catholic University of America, Washington, DC, USA
R. Bartek, A. Dominguez, R. Uniyal, A.M. Vargas Hernandez

The University of Alabama, Tuscaloosa, Alabama, USA
R. Chudasama, S.I. Cooper, D. Di Croce, S.V. Gleyzer, C. Henderson, C.U. Perez, P. Rumerio[83], C. West

Boston University, Boston, Massachusetts, USA
A. Akpinar, A. Albert, D. Arcaro, C. Cosby, Z. Demiragli, C. Erice, E. Fontanesi, D. Gastler, S. May, J. Rohlf, K. Salyer, D. Sperka, D. Spitzbart, I. Suarez, A. Tsatsos, S. Yuan

Brown University, Providence, Rhode Island, USA
G. Benelli, B. Burkle, X. Coubez[20], D. Cutts, M. Hadley, U. Heintz, J.M. Hogan[84], T. Kwon, G. Landsberg, K.T. Lau, D. Li, J. Luo, M. Narain, N. Pervan, S. Sagir[85], F. Simpson, E. Usai, W.Y. Wong, X. Yan, D. Yu, W. Zhang

University of California, Davis, Davis, California, USA
S. Abbott, J. Bonilla, C. Brainerd, R. Breedon, M. Calderon De La Barca Sanchez, M. Chertok, J. Conway, P.T. Cox, R. Erbacher, G. Haza, F. Jensen, O. Kukral, G. Mocellin, M. Mulhearn, D. Pellett, B. Regnery, Y. Yao, F. Zhang

University of California, Los Angeles, California, USA
M. Bachtis, R. Cousins, A. Datta, D. Hamilton, J. Hauser, M. Ignatenko, M.A. Iqbal, T. Lam, E. Manca, W.A. Nash, D. Saltzberg, B. Stone, V. Valuev

University of California, Riverside, Riverside, California, USA
R. Clare, J.W. Gary, M. Gordon, G. Hanson, G. Karapostoli, O.R. Long, N. Manganelli, W. Si, S. Wimpenny

University of California, San Diego, La Jolla, California, USA
J.G. Branson, S. Cittolin, S. Cooperstein, D. Diaz, J. Duarte, R. Gerosa, L. Giannini, J. Guiang, R. Kansal, V. Krutelyov, R. Lee, J. Letts, M. Masciovecchio, F. Mokhtar, M. Pieri, B.V. Sathia Narayanan, V. Sharma, M. Tadel, E. Vourliotis, F. Würthwein, Y. Xiang, A. Yagil

University of California, Santa Barbara - Department of Physics, Santa Barbara, California, USA
N. Amin, C. Campagnari, M. Citron, G. Collura, A. Dorsett, V. Dutta, J. Incandela, M. Kilpatrick, J. Kim, A.J. Li, P. Masterson, H. Mei, M. Oshiro, M. Quinnan, J. Richman, U. Sarica, R. Schmitz, F. Setti, J. Sheplock, P. Siddireddy, D. Stuart, S. Wang

California Institute of Technology, Pasadena, California, USA
A. Bornheim, O. Cerri, I. Dutta, A. Latorre, J.M. Lawhorn, J. Mao, H.B. Newman, T. Q. Nguyen, M. Spiropulu, J.R. Vlimant, C. Wang, S. Xie, R.Y. Zhu

Carnegie Mellon University, Pittsburgh, Pennsylvania, USA
J. Alison, S. An, M.B. Andrews, P. Bryant, T. Ferguson, A. Harilal, C. Liu, T. Mudholkar, S. Murthy, M. Paulini, A. Roberts, A. Sanchez, W. Terrill

University of Colorado Boulder, Boulder, Colorado, USA
J.P. Cumalat, W.T. Ford, A. Hassani, G. Karathanasis, E. MacDonald, F. Marini, A. Perloff, C. Savard, N. Schonbeck, K. Stenson, K.A. Ulmer, S.R. Wagner, N. Zipper

Cornell University, Ithaca, New York, USA
J. Alexander, S. Bright-Thonney, X. Chen, D.J. Cranshaw, J. Fan, X. Fan, D. Gadkari, S. Hogan, J. Monroy, J.R. Patterson, D. Quach, J. Reichert, M. Reid, A. Ryd, J. Thom, P. Wittich, R. Zou

Fermi National Accelerator Laboratory, Batavia, Illinois, USA
M. Albrow, M. Alyari, G. Apollinari, A. Apresyan, L.A.T. Bauerdick, D. Berry, J. Berryhill, P.C. Bhat, K. Burkett, J.N. Butler, A. Canepa, G.B. Cerati, H.W.K. Cheung, F. Chlebana, K.F. Di Petrillo, J. Dickinson, V.D. Elvira, Y. Feng, J. Freeman, A. Gandrakota, Z. Gecse, L. Gray, D. Green, S. Grünendahl, D. Guerrero, O. Gutsche, R.M. Harris, R. Heller, T.C. Herwig, J. Hirschauer, L. Horyn, B. Jayatilaka, S. Jindariani, M. Johnson, U. Joshi, T. Klijnsma, B. Klima, K.H.M. Kwok, S. Lammel, D. Lincoln, R. Lipton, T. Liu, C. Madrid, K. Maeshima, C. Mantilla, D. Mason, P. McBride, P. Merkel, S. Mrenna, S. Nahn, J. Ngadiuba, D. Noonan, V. Papadimitriou, N. Pastika, K. Pedro, C. Pena[86], F. Ravera, A. Reinsvold Hall[87], L. Ristori, E. Sexton-Kennedy, N. Smith, A. Soha, L. Spiegel, J. Strait, L. Taylor, S. Tkaczyk, N.V. Tran, L. Uplegger, E.W. Vaandering, I. Zoi

University of Florida, Gainesville, Florida, USA
P. Avery, D. Bourilkov, L. Cadamuro, P. Chang, V. Cherepanov, R.D. Field, E. Koenig, J. Konigsberg, A. Korytov, E. Kuznetsova[88], K.H. Lo, K. Matchev, N. Menendez, G. Mitselmakher, A. Muthirakalayil Madhu, N. Rawal, D. Rosenzweig, S. Rosenzweig, K. Shi, J. Wang, Z. Wu

Florida State University, Tallahassee, Florida, USA
T. Adams, A. Askew, N. Bower, R. Habibullah, V. Hagopian, T. Kolberg, G. Martinez, H. Prosper, O. Viazlo, M. Wulansatiti, R. Yohay, J. Zhang

Florida Institute of Technology, Melbourne, Florida, USA
M.M. Baarmand, S. Butalla, T. Elkafrawy[52], M. Hohlmann, R. Kumar Verma, M. Rahmani, F. Yumiceva

University of Illinois Chicago, Chicago, USA, Chicago, USA
M.R. Adams, R. Cavanaugh, S. Dittmer, O. Evdokimov, C.E. Gerber, D.J. Hofman, D. S. Lemos, A.H. Merrit, C. Mills, G. Oh, T. Roy, S. Rudrabhatla, M.B. Tonjes, N. Varelas, X. Wang, Z. Ye, J. Yoo

The University of Iowa, Iowa City, Iowa, USA
M. Alhusseini, K. Dilsiz[89], L. Emediato, G. Karaman, O.K. Köseyan, J.-P. Merlo, A. Mestvirishvili[90], J. Nachtman, O. Neogi, H. Ogul[91], Y. Onel, A. Penzo, C. Snyder, E. Tiras[92]

Johns Hopkins University, Baltimore, Maryland, USA
O. Amram, B. Blumenfeld, L. Corcodilos, J. Davis, A.V. Gritsan, S. Kyriacou, P. Maksimovic, J. Roskes, S. Sekhar, M. Swartz, T.Á. Vámi

The University of Kansas, Lawrence, Kansas, USA
A. Abreu, L.F. Alcerro Alcerro, J. Anguiano, P. Baringer, A. Bean, Z. Flowers, T. Isidori, J. King, G. Krintiras, M. Lazarovits, C. Le Mahieu, C. Lindsey, J. Marquez, N. Minafra, M. Murray, M. Nickel, C. Rogan, C. Royon, R. Salvatico, S. Sanders, C. Smith, Q. Wang, G. Wilson

Kansas State University, Manhattan, Kansas, USA

B. Allmond, S. Duric, A. Ivanov, K. Kaadze, A. Kalogeropoulos, D. Kim, Y. Maravin, T. Mitchell, A. Modak, K. Nam, D. Roy

Lawrence Livermore National Laboratory, Livermore, California, USA
F. Rebassoo, D. Wright

University of Maryland, College Park, Maryland, USA
E. Adams, A. Baden, O. Baron, A. Belloni, A. Bethani, S.C. Eno, N.J. Hadley, S. Jabeen, R.G. Kellogg, T. Koeth, Y. Lai, S. Lascio, A.C. Mignerey, S. Nabili, C. Palmer, C. Papageorgakis, L. Wang, K. Wong

Massachusetts Institute of Technology, Cambridge, Massachusetts, USA
D. Abercrombie, W. Busza, I.A. Cali, Y. Chen, M. D'Alfonso, J. Eysermans, C. Freer, G. Gomez-Ceballos, M. Goncharov, P. Harris, M. Hu, D. Kovalskyi, J. Krupa, Y.-J. Lee, K. Long, C. Mironov, C. Paus, D. Rankin, C. Roland, G. Roland, Z. Shi, G.S.F. Stephans, J. Wang, Z. Wang, B. Wyslouch, T. J. Yang

University of Minnesota, Minneapolis, Minnesota, USA
R.M. Chatterjee, B. Crossman, J. Hiltbrand, B.M. Joshi, C. Kapsiak, M. Krohn, Y. Kubota, J. Mans, M. Revering, R. Rusack, R. Saradhy, N. Schroeder, N. Strobbe, M.A. Wadud

University of Mississippi, Oxford, Mississippi, USA
L.M. Cremaldi

University of Nebraska-Lincoln, Lincoln, Nebraska, USA
K. Bloom, M. Bryson, D.R. Claes, C. Fangmeier, L. Finco, F. Golf, C. Joo, R. Kamalieddin, I. Kravchenko, I. Reed, J.E. Siado, G.R. Snow†, W. Tabb, A. Wightman, F. Yan, A.G. Zecchinelli

State University of New York at Buffalo, Buffalo, New York, USA
G. Agarwal, H. Bandyopadhyay, L. Hay, I. Iashvili, A. Kharchilava, C. McLean, M. Morris, D. Nguyen, J. Pekkanen, S. Rappoccio, A. Williams

Northeastern University, Boston, Massachusetts, USA
G. Alverson, E. Barberis, Y. Haddad, Y. Han, A. Krishna, J. Li, J. Lidrych, G. Madigan, B. Marzocchi, D.M. Morse, V. Nguyen, T. Orimoto, A. Parker, L. Skinnari, A. Tishelman-Charny, T. Wamorkar, B. Wang, A. Wisecarver, D. Wood

Northwestern University, Evanston, Illinois, USA
S. Bhattacharya, J. Bueghly, Z. Chen, A. Gilbert, K.A. Hahn, Y. Liu, N. Odell, M.H. Schmitt, M. Velasco

University of Notre Dame, Notre Dame, Indiana, USA
R. Band, R. Bucci, M. Cremonesi, A. Das, R. Goldouzian, M. Hildreth, K. Hurtado Anampa, C. Jessop, K. Lannon, J. Lawrence, N. Loukas, L. Lutton, J. Mariano, N. Marinelli, I. Mcalister, T. McCauley, C. Mcgrady, K. Mohrman, C. Moore, Y. Musienko[11], R. Ruchti, A. Townsend, M. Wayne, H. Yockey, M. Zarucki, L. Zygala

The Ohio State University, Columbus, Ohio, USA
B. Bylsma, M. Carrigan, L.S. Durkin, C. Hill, M. Joyce, A. Lesauvage, M. Nunez Ornelas, K. Wei, B.L. Winer, B. R. Yates

Princeton University, Princeton, New Jersey, USA
F.M. Addesa, P. Das, G. Dezoort, P. Elmer, A. Frankenthal, B. Greenberg, N. Haubrich, S. Higginbotham, G. Kopp, S. Kwan, D. Lange, A. Loeliger, D. Marlow, I. Ojalvo, J. Olsen, D. Stickland, C. Tully

University of Puerto Rico, Mayaguez, Puerto Rico, USA
S. Malik, S. Norberg

Purdue University, West Lafayette, Indiana, USA
A.S. Bakshi, V.E. Barnes, R. Chawla, S. Das, L. Gutay, M. Jones, A.W. Jung, D. Kondratyev, A.M. Koshy, M. Liu, G. Negro, N. Neumeister, G. Paspalaki, S. Piperov, A. Purohit, J.F. Schulte, M. Stojanovic[14], J. Thieman, F. Wang, R. Xiao, W. Xie

Purdue University Northwest, Hammond, Indiana, USA
J. Dolen, N. Parashar

Rice University, Houston, Texas, USA
D. Acosta, A. Baty, T. Carnahan, S. Dildick, K.M. Ecklund, P.J. Fernández Manteca, S. Freed, P. Gardner, F.J.M. Geurts, A. Kumar, W. Li, B.P. Padley, R. Redjimi, J. Rotter, S. Yang, E. Yigitbasi, Y. Zhang

University of Rochester, Rochester, New York, USA
A. Bodek, P. de Barbaro, R. Demina, J.L. Dulemba, C. Fallon, M. Galanti, A. Garcia-Bellido, O. Hindrichs, A. Khukhunaishvili, P. Parygin, E. Popova, R. Taus, G.P. Van Onsem

The Rockefeller University, New York, New York, USA
K. Goulianos

Rutgers, The State University of New Jersey, Piscataway, New Jersey, USA
B. Chiarito, J.P. Chou, Y. Gershtein, E. Halkiadakis, A. Hart, M. Heindl, D. Jaroslawski, O. Karacheban[23], I. Laflotte, A. Lath, R. Montalvo, K. Nash, M. Osherson, H. Routray, S. Salur, S. Schnetzer, S. Somalwar, R. Stone, S.A. Thayil, S. Thomas, H. Wang

University of Tennessee, Knoxville, Tennessee, USA
H. Acharya, A.G. Delannoy, S. Fiorendi, T. Holmes, E. Nibigira, S. Spanier

Texas A&M University, College Station, Texas, USA
O. Bouhali[93], M. Dalchenko, A. Delgado, R. Eusebi, J. Gilmore, T. Huang, T. Kamon[94], H. Kim, S. Luo, S. Malhotra, R. Mueller, D. Overton, D. Rathjens, A. Safonov

Texas Tech University, Lubbock, Texas, USA
N. Akchurin, J. Damgov, V. Hegde, K. Lamichhane, S.W. Lee, T. Mengke, S. Muthumuni, T. Peltola, I. Volobouev, A. Whitbeck

Vanderbilt University, Nashville, Tennessee, USA
E. Appelt, S. Greene, A. Gurrola, W. Johns, A. Melo, F. Romeo, P. Sheldon, S. Tuo, J. Velkovska, J. Viinikainen

University of Virginia, Charlottesville, Virginia, USA
B. Cardwell, B. Cox, G. Cummings, J. Hakala, R. Hirosky, A. Ledovskoy, A. Li, C. Neu, C.E. Perez Lara, B. Tannenwald

Wayne State University, Detroit, Michigan, USA
P.E. Karchin, N. Poudyal

University of Wisconsin - Madison, Madison, Wisconsin, USA
A. Aravind, S. Banerjee, K. Black, T. Bose, S. Dasu, I. De Bruyn, P. Everaerts, C. Galloni, H. He, M. Herndon, A. Herve, C.K. Koraka, A. Lanaro, R. Loveless, J. Madhusudanan Sreekala, A. Mallampalli, A. Mohammadi, S. Mondal, G. Parida, D. Pinna, A. Savin, V. Shang, V. Sharma, W.H. Smith, D. Teague, H.F. Tsoi, W. Vetens, A. Warden

Authors affiliated with an institute or an international laboratory covered by a cooperation agreement with CERN
S. Afanasiev, V. Andreev, Yu. Andreev, T. Aushev, M. Azarkin, A. Babaev, A. Belyaev, V. Blinov[95], E. Boos, V. Borshch, D. Budkouski, V. Bunichev, M. Chadeeva[95], V. Chekhovsky, R. Chistov[95], A. Dermenev, T. Dimova[95], I. Dremin, M. Dubinin[86], L. Dudko, V. Epshteyn, G. Gavrilov, V. Gavrilov, S. Gninenko, V. Golovtcov, N. Golubev, I. Golutvin, I. Gorbunov, A. Gribushin, Y. Ivanov, V. Kachanov, L. Kardapoltsev[95], V. Karjavine, A. Karneyeu, V. Kim[95], M. Kirakosyan, D. Kirpichnikov, M. Kirsanov, V. Klyukhin, O. Kodolova[96], D. Konstantinov, V. Korenkov, A. Kozyrev[95], N. Krasnikov, A. Lanev, P. Levchenko, A. Litomin, N. Lychkovskaya, V. Makarenko, A. Malakhov, V. Matveev[95], V. Murzin, A. Nikitenko[97], S. Obraztsov, A. Oskin, I. Ovtin[95], V. Palichik, V. Perelygin, M. Perfilov, S. Petrushanko, S. Polikarpov[95], V. Popov, O. Radchenko[95], M. Savina, V. Savrin, V. Shalaev, S. Shmatov, S. Shulha, Y. Skovpen[95], S. Slabospitskii, V. Smirnov, D. Sosnov, V. Sulimov, E. Tcherniaev, A. Terkulov, O. Teryaev, I. Tlisova, A. Toropin, L. Uvarov, A. Uzunian, A. Vorobyev, N. Voytishin, B.S. Yuldashev[98], A. Zarubin, I. Zhizhin, A. Zhokin

†: Deceased
[1]Also at TU Wien, Vienna, Austria
[2]Also at Institute of Basic and Applied Sciences, Faculty of Engineering, Arab Academy for Science, Technology and Maritime Transport, Alexandria, Egypt
[3]Also at Université Libre de Bruxelles, Bruxelles, Belgium
[4]Also at Universidade Estadual de Campinas, Campinas, Brazil
[5]Also at Federal University of Rio Grande do Sul, Porto Alegre, Brazil
[6]Also at UFMS, Nova Andradina, Brazil
[7]Also at University of Chinese Academy of Sciences, Beijing, China
[8]Also at Nanjing Normal University, Nanjing, China
[9]Now at The University of Iowa, Iowa City, Iowa, USA
[10]Also at University of Chinese Academy of Sciences, Beijing, China
[11]Also at an institute or an international laboratory covered by a cooperation agreement with CERN
[12]Now at British University in Egypt, Cairo, Egypt
[13]Now at Cairo University, Cairo, Egypt
[14]Also at Purdue University, West Lafayette, Indiana, USA
[15]Also at Université de Haute Alsace, Mulhouse, France
[16]Also at Department of Physics, Tsinghua University, Beijing, China
[17]Also at The University of the State of Amazonas, Manaus, Brazil
[18]Also at Erzincan Binali Yildirim University, Erzincan, Turkey
[19]Also at University of Hamburg, Hamburg, Germany
[20]Also at RWTH Aachen University, III. Physikalisches Institut A, Aachen, Germany

[21]Also at Isfahan University of Technology, Isfahan, Iran
[22]Also at Bergische University Wuppertal (BUW), Wuppertal, Germany
[23]Also at Brandenburg University of Technology, Cottbus, Germany
[24]Also at Forschungszentrum Jülich, Juelich, Germany
[25]Also at CERN, European Organization for Nuclear Research, Geneva, Switzerland
[26]Also at Physics Department, Faculty of Science, Assiut University, Assiut, Egypt
[27]Also at Karoly Robert Campus, MATE Institute of Technology, Gyongyos, Hungary
[28]Also at Wigner Research Centre for Physics, Budapest, Hungary
[29]Also at Institute of Physics, University of Debrecen, Debrecen, Hungary
[30]Also at Institute of Nuclear Research ATOMKI, Debrecen, Hungary
[31]Now at Universitatea Babes-Bolyai - Facultatea de Fizica, Cluj-Napoca, Romania
[32]Also at Faculty of Informatics, University of Debrecen, Debrecen, Hungary
[33]Also at Punjab Agricultural University, Ludhiana, India
[34]Also at UPES - University of Petroleum and Energy Studies, Dehradun, India
[35]Also at University of Visva-Bharati, Santiniketan, India
[36]Also at University of Hyderabad, Hyderabad, India
[37]Also at Indian Institute of Science (IISc), Bangalore, India
[38]Also at Indian Institute of Technology (IIT), Mumbai, India
[39]Also at IIT Bhubaneswar, Bhubaneswar, India
[40]Also at Institute of Physics, Bhubaneswar, India
[41]Also at Deutsches Elektronen-Synchrotron, Hamburg, Germany
[42]Now at Department of Physics, Isfahan University of Technology, Isfahan, Iran
[43]Also at Sharif University of Technology, Tehran, Iran
[44]Also at Department of Physics, University of Science and Technology of Mazandaran, Behshahr, Iran
[45]Also at Helwan University, Cairo, Egypt
[46]Also at Italian National Agency for New Technologies, Energy and Sustainable Economic Development, Bologna, Italy
[47]Also at Centro Siciliano di Fisica Nucleare e di Struttura Della Materia, Catania, Italy
[48]Also at Università degli Studi Guglielmo Marconi, Roma, Italy
[49]Also at Scuola Superiore Meridionale, Università di Napoli 'Federico II', Napoli, Italy
[50]Also at Fermi National Accelerator Laboratory, Batavia, Illinois, USA
[51]Also at Università di Napoli 'Federico II', Napoli, Italy
[52]Also at Ain Shams University, Cairo, Egypt
[53]Also at Consiglio Nazionale delle Ricerche - Istituto Officina dei Materiali, Perugia, Italy
[54]Also at Riga Technical University, Riga, Latvia
[55]Also at Department of Applied Physics, Faculty of Science and Technology, Universiti Kebangsaan Malaysia, Bangi, Malaysia
[56]Also at Consejo Nacional de Ciencia y Tecnología, Mexico City, Mexico
[57]Also at IRFU, CEA, Université Paris-Saclay, Gif-sur-Yvette, France
[58]Also at Faculty of Physics, University of Belgrade, Belgrade, Serbia
[59]Also at Trincomalee Campus, Eastern University, Sri Lanka, Nilaveli, Sri Lanka
[60]Also at INFN Sezione di Pavia, Università di Pavia, Pavia, Italy
[61]Also at National and Kapodistrian University of Athens, Athens, Greece
[62]Also at Ecole Polytechnique Fédérale Lausanne, Lausanne, Switzerland
[63]Also at Universität Zürich, Zurich, Switzerland
[64]Also at Stefan Meyer Institute for Subatomic Physics, Vienna, Austria
[65]Also at Laboratoire d'Annecy-le-Vieux de Physique des Particules, IN2P3-CNRS, Annecy-le-Vieux, France

[66]Also at Near East University, Research Center of Experimental Health Science, Mersin, Turkey
[67]Also at Konya Technical University, Konya, Turkey
[68]Also at Izmir Bakircay University, Izmir, Turkey
[69]Also at Adiyaman University, Adiyaman, Turkey
[70]Also at Istanbul Gedik University, Istanbul, Turkey
[71]Also at Necmettin Erbakan University, Konya, Turkey
[72]Also at Bozok Universitetesi Rektörlügü, Yozgat, Turkey
[73]Also at Marmara University, Istanbul, Turkey
[74]Also at Milli Savunma University, Istanbul, Turkey
[75]Also at Kafkas University, Kars, Turkey
[76]Also at Istanbul University - Cerrahpasa, Faculty of Engineering, Istanbul, Turkey
[77]Also at Yildiz Technical University, Istanbul, Turkey
[78]Also at Vrije Universiteit Brussel, Brussel, Belgium
[79]Also at School of Physics and Astronomy, University of Southampton, Southampton, United Kingdom
[80]Also at University of Bristol, Bristol, United Kingdom
[81]Also at IPPP Durham University, Durham, United Kingdom
[82]Also at Monash University, Faculty of Science, Clayton, Australia
[83]Also at Università di Torino, Torino, Italy
[84]Also at Bethel University, St. Paul, Minnesota, USA
[85]Also at Karamanoğlu Mehmetbey University, Karaman, Turkey
[86]Also at California Institute of Technology, Pasadena, California, USA
[87]Also at United States Naval Academy, Annapolis, Maryland, USA
[88]Also at University of Florida, Gainesville, Florida, USA
[89]Also at Bingol University, Bingol, Turkey
[90]Also at Georgian Technical University, Tbilisi, Georgia
[91]Also at Sinop University, Sinop, Turkey
[92]Also at Erciyes University, Kayseri, Turkey
[93]Also at Texas A&M University at Qatar, Doha, Qatar
[94]Also at Kyungpook National University, Daegu, Korea
[95]Also at another institute or international laboratory covered by a cooperation agreement with CERN
[96]Also at Yerevan Physics Institute, Yerevan, Armenia
[97]Also at Imperial College, London, United Kingdom
[98]Also at Institute of Nuclear Physics of the Uzbekistan Academy of Sciences, Tashkent, Uzbekistan